

Determination of the restoration effect on the structural behavior of masonry arch bridges

A.C. Altunisik*, A. Bayraktar and A.F. Genc

Department of Civil Engineering, Karadeniz Technical University, Trabzon, Turkey

(Received June 5, 2014, Revised August 22, 2014, Accepted August 31, 2014)

Abstract. In this paper, it is aimed to investigate the restoration effect on the structural behavior of masonry arch bridges. Dandalaz masonry arch bridge located on the 4km east of Karacasu town of Aydın, Turkey is selected as a numerical example. The construction year of the bridge is not fully known, but the bridge is dated back to 15th century. Considering the current situation, it can be easily seen that the structural elements such as arch, side walls and timber blocks are heavily damaged and the bridge is unserviceable. Firstly finite element model of the bridge is constituted to reflect the current situation (before restoration) using building survey drawings. After, restoration project is explained and finite element model is reconstituted (after restoration). The structural responses of the bridge are obtained before and after restoration under dead load, live load and dynamic earthquake loads. For both conditions, maximum displacements, maximum-minimum principal stresses and maximum-minimum elastic strains are given with detail using contours diagrams and compared with each other to determine the restoration effect. From the study, it can be seen that the maximum internal forces are consisted under dynamic loads before and after restoration. Also, the restoration projects and studies have important and positive effects on the structural response of the bridge to transfer these structures to future.

Keywords: dynamic earthquake loads; finite element model; masonry arch bridge; structural response; restoration effect

1. Introduction

Preservation of historical structures is considered a fundamental issue in the cultural life of modern societies as a consequence of collapsing some of them in the world in the last decades (Bayraktar *et al.* 2009a). Historical masonry bridges are one of the primary engineering structures constructed by people. There are a lot of historical bridges constructed in various sizes, styles and spans all over the world. Some of them are nearly as old as a couple of thousands years. These bridges are very important part of culture heritage of countries and they should be preserved well for the next generation.

There are a lot of historical arch bridges constructed in various sizes, styles and spans in Turkey. Nearly 1550 recorded historical bridges exist in Turkey built different areas and times. They were built for different purposes such as social and economical as well as strategic aims. In spite of the fact that these bridges were designed to carry only pedestrian and horse loads, in these days as a

*Corresponding author, Associate Professor, E-mail: ahmetcan8284@hotmail.com

result of modern civilization most of them are used for traffic. For conservation, restoration and reinforcement of these structures, their structural behaviors need to be known well and so dynamics characteristics of them have to be identified. Consequently, well defined numerical analysis method for these kinds of structures is needed (Bayraktar *et al.* 2009b).

In the last decade, the conservation and the structural safety assessment of ancient masonry structures such as bridges have become of increasing concern, probably as a consequence of some events registered in Europe, like the failures of the Prestwood bridge (Betti *et al.* 2007), cracks in the four span arch bridge in Urnieta, Spain (Leon and Espejo 2007), failures of the Palu bridge in Turkey (Gonen *et al.* 2013), collapse of the Mostar bridge in Bosnia and Herzegovina. Examples of recent investigations and restoration applications include well-known bridges, such as Uzunköprü, Malabadi, Çobandede, Göderni and Dandalaz Bridges in Turkey (Ural *et al.* 2008), the Venta Bridge in Kuldiga (Paegliti and Paegliti 2009), the Wisconsin Avenue Bridge in Milwaukee. These investigations involve both analytical and experimental methods including several tasks: field survey for determination of the dynamic characteristics of structures, finite element modeling, theoretical analysis and laboratory tests on samples.

There are many studies in literature including both analytical and experimental investigations of masonry arch bridges structures. Tao *et al.* (2011) determined to the behaviour of a masonry arch bridge repaired using fibre-reinforced polymer composites. Milani and Lourenço (2012) attained to the non-linear static behavior of masonry bridges by using of three dimensional finite element numerical codes. Smoljanovic *et al.* (2013) presented the performance of a combined finite discrete element method for the material and geometric nonlinear analysis of the structural response of dry stone masonry structures under monotonic, cyclic and seismic loads. Pela *et al.* (2013) compared the seismic assessment procedures for masonry arch bridges. Gonen *et al.* (2013) examined the failure results in the structural system of the bridge. Also, the effect of water to structural elements was evaluated. Reccia *et al.* (2014) suggested the full 3D homogenization approach to investigate the behavior of masonry arch bridges. Besides these studies, it can be seen that there is no enough studies about the determination and comparison of the static and dynamic structural response of historical masonry arch bridges.

2. Numerical application

Dandalaz masonry arch bridge is located on the Karacasu-Tavas state highway and Dandalaz brook in the 4km east of Karacasu town of Aydın, Turkey. The construction year of the bridge is not fully known, but the bridge is dated back to 15th century. The arch stones of the bridge, which has hoop-shapes arch and single span, are made of processed rectangular limestone. The side walls especially lower parts consists of rough stones. Sequential rubble stone covering can be seen in the other parts of the bridges instead of the pouring stones during repairs.

The main structural elements of the bridge (stone arch, side walls and timber block) have heavily damaged and have not been repaired yet. For this reason, the bridge is now unserviceable. After restoration projects and studies, it is planned to opening of the bridge only for pedestrian crossings. Some views of Dandalaz Bridge are shown in Fig. 1.

The bridge has a single arch. The total length of bridge is 35.93 m, the maximum span of bridge arch is 19.2 m, the maximum height of the arch is 9.2 m, the distance between water level and inner surface of bridge arch is 20.16 m, and the wide of the deck is 6.20 m, respectively. The historical bridge has a stone arch; radius and thickness of which are 10.2 m and 85 cm,

respectively. In addition, thickness of the side walls is 40 cm and there is a timber block between the walls, wide of which is 5.4 m. Height of the side walls at both side 5.75 m and 5.18 m, respectively. There are 40x100 cm dimensional parapets on the both side of the bridge deck. Asphalt pavement is made on the original flooring of bridge deck. Also, it is seen that steel tubes are upholstered on the bridge deck to ensure the water transmission in the town.

3. Determination of the material properties

Dandalaz Bridge is a stone arch bridge. Even if this type of bridges are generally expressed as a stone, different type of materials such as stone, steel and wood can be used for several purposes in the structural systems. The arch and side walls are build using cut stone and different types of stone, respectively. Lime-based mortar is used in the structural carrier elements as a binding material. Also, cement mortar is used in some places. As other historical masonry arch bridge, the timber blocks between side walls are composed to variable sizes of limestone, sand and gravel. Parapets are made from cut stone.

To determine the mechanical properties of materials used in the bridge, stone and mortar samples taken from the bridge are tested in the laboratory. As a result of the experimental studies, the mechanical properties are obtained and they are used to compare and control the displacements, stresses and strains obtained from the finite element analysis. The compressive strength and weight per unit volume are determined as 50MPa and 2200-2400 kg/m³ for stones, respectively. Also, the compressive strength of the mortar is defined as 5-7MPa. Some views of the stone and mortar samples, experimental studies and experimental results are given in Fig. 2.



Fig. 1 Some views of Dandalaz historical masonry arch bridge

bridge before and after restorations are constituted using ANSYS software (ANSYS 2008).

The analyses performed for this purpose are grouped as follows:

- 1) Finite element analysis of the bridge under current situation (before restoration)
 - Structural response under dead load
 - Structural response under dead load and live loads
 - Structural response under dead load, live loads and dynamic (earthquake) loads
- 2) Finite element analysis of the bridge after restoration
 - Structural response under dead load
 - Structural response under dead load and live loads
 - Structural response under dead load, live loads and dynamic (earthquake) loads

SOLID186 solid elements are used in the finite element models of the bridges. The element had 20 node and three degrees of freedom per node: translations in the nodal x, y, and z directions. In addition it had the capability of plasticity, elasticity, creep, stress stiffening, large deflection, and large strains (ANSYS 2008). When the structural solid geometry property of the SOLID186 element is examined, it can be seen that the elements appears to be made of tetrahedral, pyramid or prism options in the finite element mesh model of the bridge. A schematic of the SOLID186 element is shown in Fig. 3.

4.1 Finite element analysis of the bridge under current situation (before restoration)

In the finite element model of the bridge under current situation (before restoration), damaged elements are taken into account. 3D finite element model of the bridge constituted using ANSYS software shown in Fig. 4. In the finite element model, three dimensional solid elements have been used. This model consists of 141266 nodes and 95193 mesh elements. All analyses are performed as linear elastic. As boundary conditions, all of freedoms under the bridge abutments and at the side walls are considered as fixed.

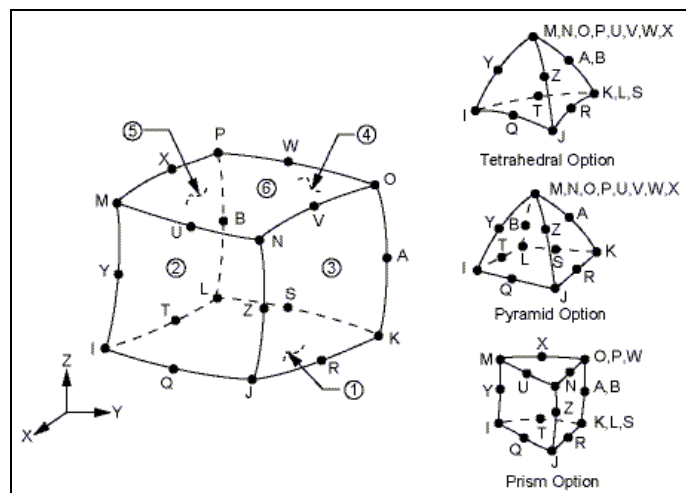


Fig. 3 Structural solid geometry of SOLID186 element

Table 1 Material properties considered in the analytical analysis

Structural Elements	Material Properties			
	Modulus of Elasticity (N/m^2)		Poisson Ratio (-)	Density (kg/m^3)
	Un-damaged	Damaged		
Arches	1.6E10	0.64E10	0.30	2000
Side Walls	1.6E10	0.64E10	0.30	2000
Timber Blocks	7.5E09	2.25E09	0.30	1200
Parapets	1.6E10	0.64E10	0.30	2000
Ground	2.0E10	2.0E10	0.35	2500

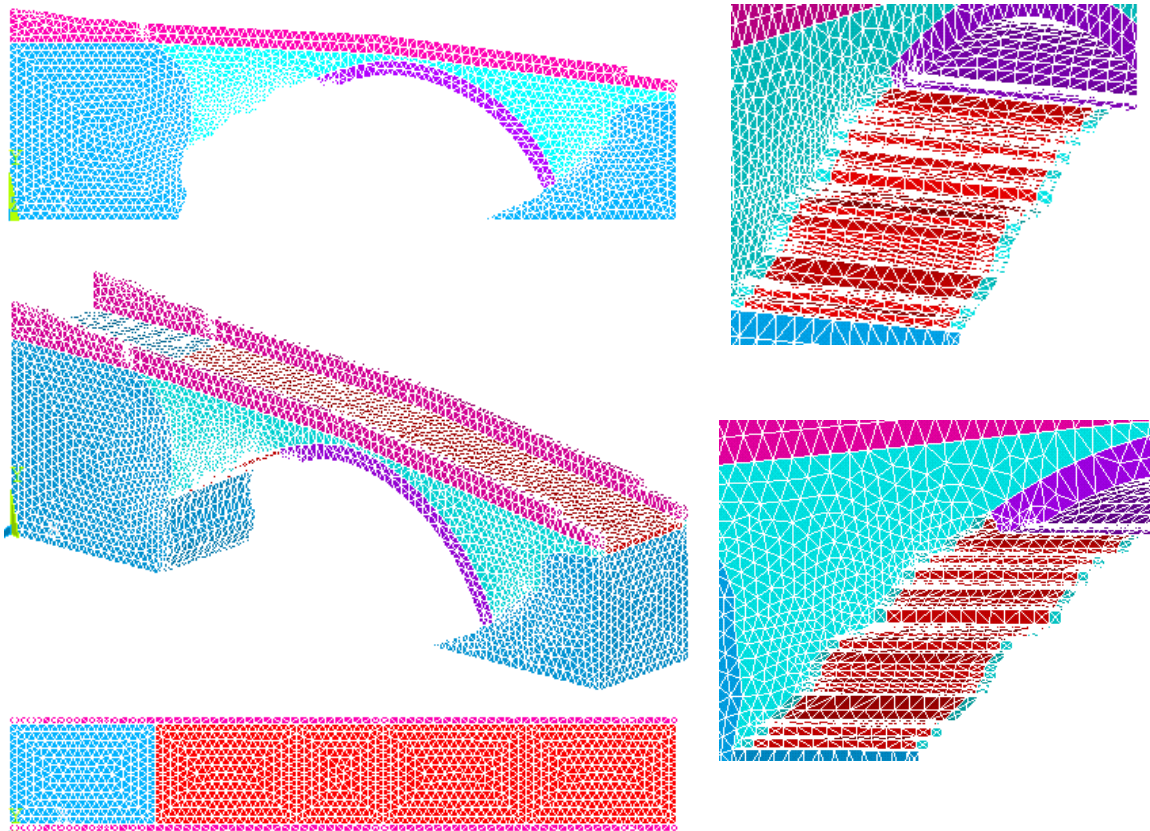


Fig. 4 Finite element model of Dandalaz masonry arch bridge

In the analysis of historical structures, selection of the material properties accurately is very important. Because of difficulties to determine the material properties of such kind of structures, similar studies in the literature have been searched and material properties considered in analysis are determined (Frunzio *et al.* 2001, Toker and Unay 2004, Bayraktar *et al.* 2007, Brencich and Sabia 2008). The material properties considered in the analysis of the bridge are given in Table 1. The values of Elasticity Modulus given in Table 1 can be taken into account for un-damaged conditions in structural elements. But, in the current situation (before restoration) of Dandalaz Bridge, some damaged conditions such as the ruptures, deteriorations and cracks are identified. So, the material properties are reduced within the acceptable limits considering related articles, thesis and laboratory studies.

4.1.1 Structural response under dead load

The maximum vertical displacements contour of the bridge before restorations under dead load is shown in Fig. 5. This represents the distribution of the peak values reached by the maximum displacement at each point within the sections. It is seen that displacements decrease from the middle point of the bridge arch to side supports and foots. The maximum displacement occurs at the middle of the arch (damaged sections) as 1.40 mm.

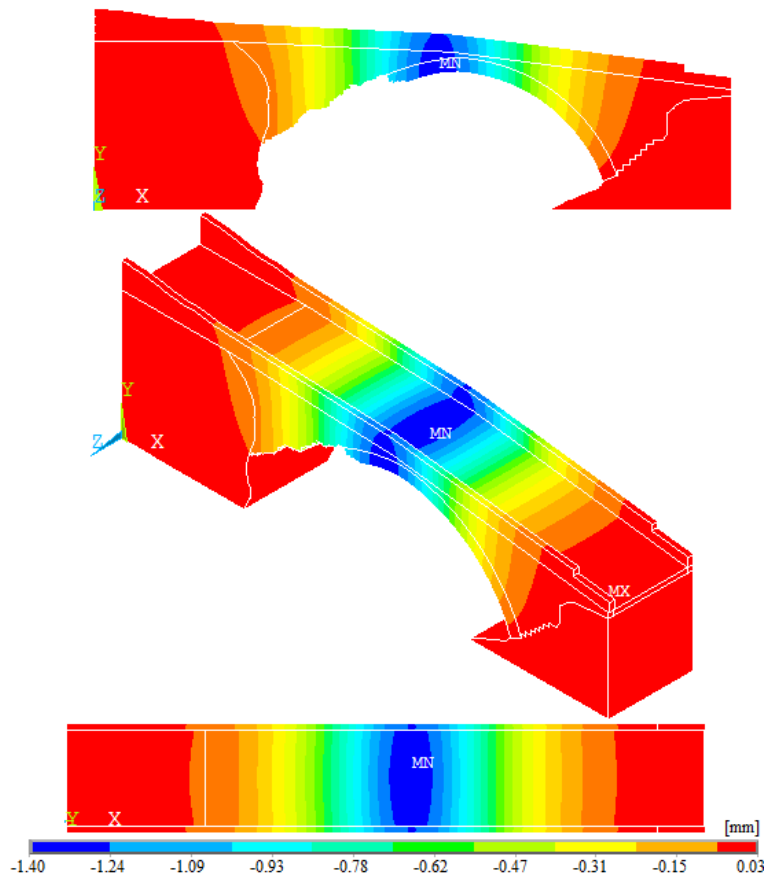


Fig. 5 Maximum displacement contours of the masonry bridge before restoration under dead load

The maximum tensile stress contour of the bridge before restorations under dead load is shown in Fig. 6. This stress contour represents the distribution of the peak values reached by the maximum tensile stress at each point within the section. It is seen that maximum values of the tensile stresses consist on the contact points between bridge and side slopes as a 0.58 MPa, locally. Also, some stress accumulations regions are determined on the side walls, arches and parapets valued at 0.28 MPa. Excluding these sections, maximum tensile stresses are attained as 0.08 MPa.

The maximum compressive stress contour of the bridge before restorations under dead load is shown in Fig. 7. This stress contour represents the distribution of the peak values reached by the maximum compressive stress at each point within the section. It is seen that maximum values of the compressive stresses consist on the lower parts of the damaged side walls and arches as a 1.70 MPa. Also, some stress accumulations regions are determined on the side walls and arches (especially right side of the arches and near of the supports) valued at 1.08 MPa. Excluding these sections, maximum compressive stresses are attained as 0.48 MPa.

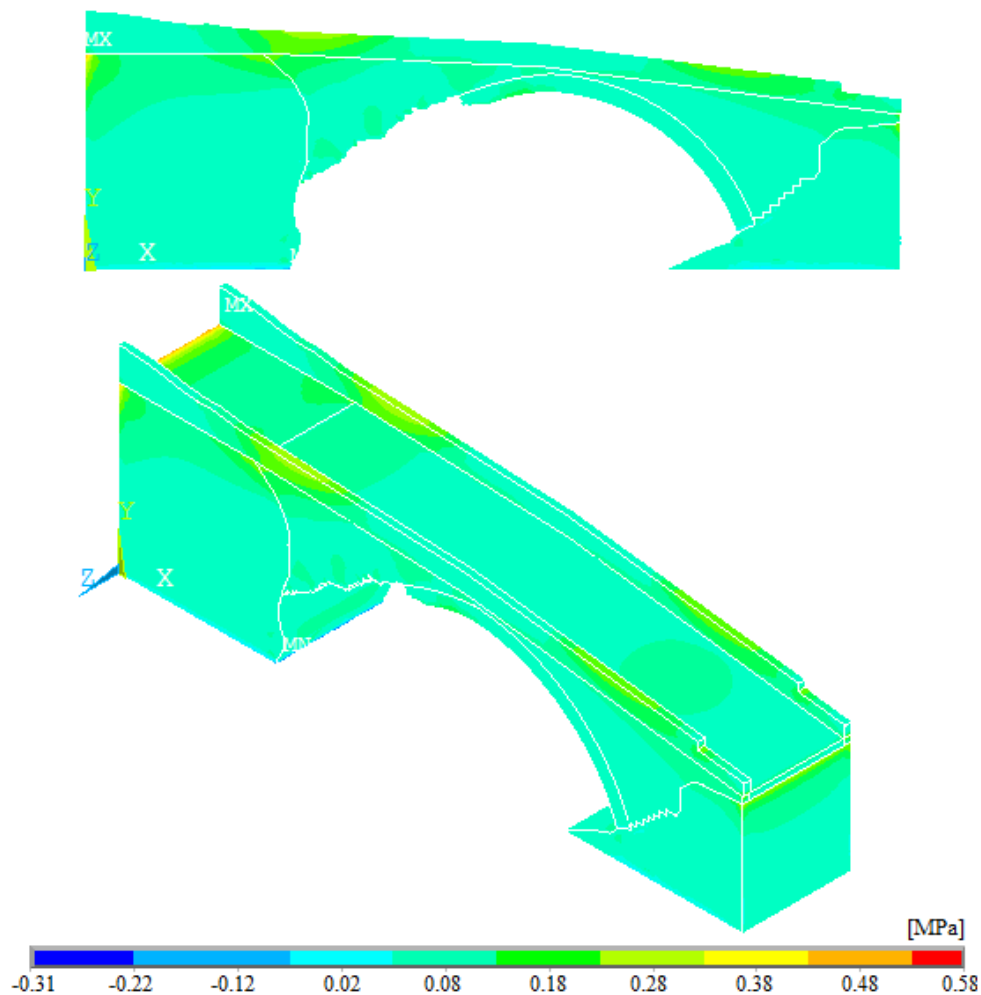


Fig. 6 Maximum tensile stress of the masonry bridge before restoration under dead load

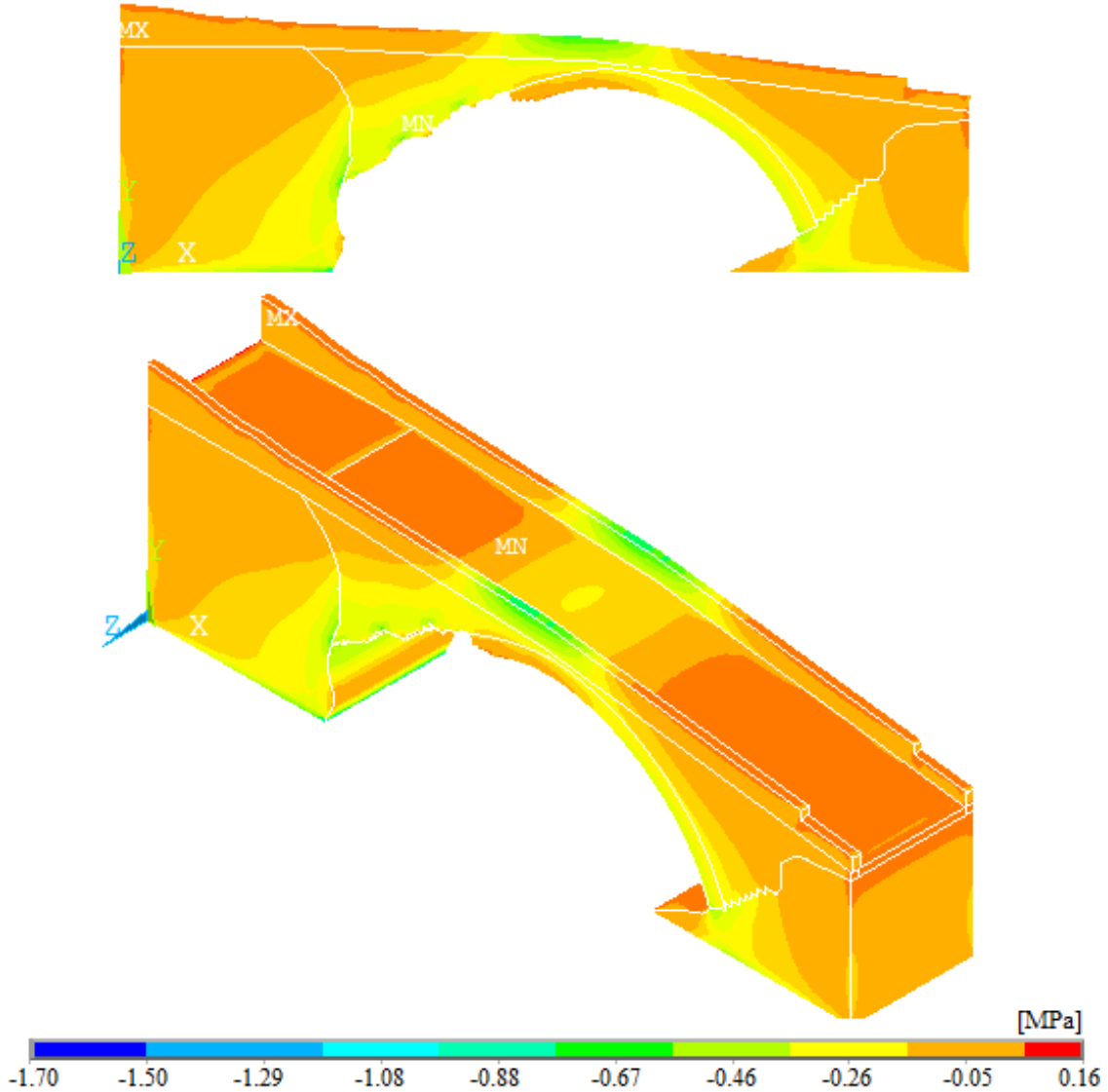


Fig. 7 Maximum compressive stress of the masonry bridge before restoration under dead load

The maximum and minimum elastic strains contours of the bridge before restorations under dead load are shown in Fig. 8. It is seen that maximum and minimum values of the elastic strains attained as $0.67\text{E-}4$ and $0.24\text{E-}3$, respectively. Also, some strain accumulations regions are determined for maximum elastic strains on the damaged side walls, lower and inner part of the arches, and some points on the roadway valued at $0.30\text{E-}4$. As well as, some strain accumulations regions are attained for minimum elastic strains on the inner part of the arches, some points of parapets and lower sections of side walls near the arch valued at $0.08\text{E-}3$.

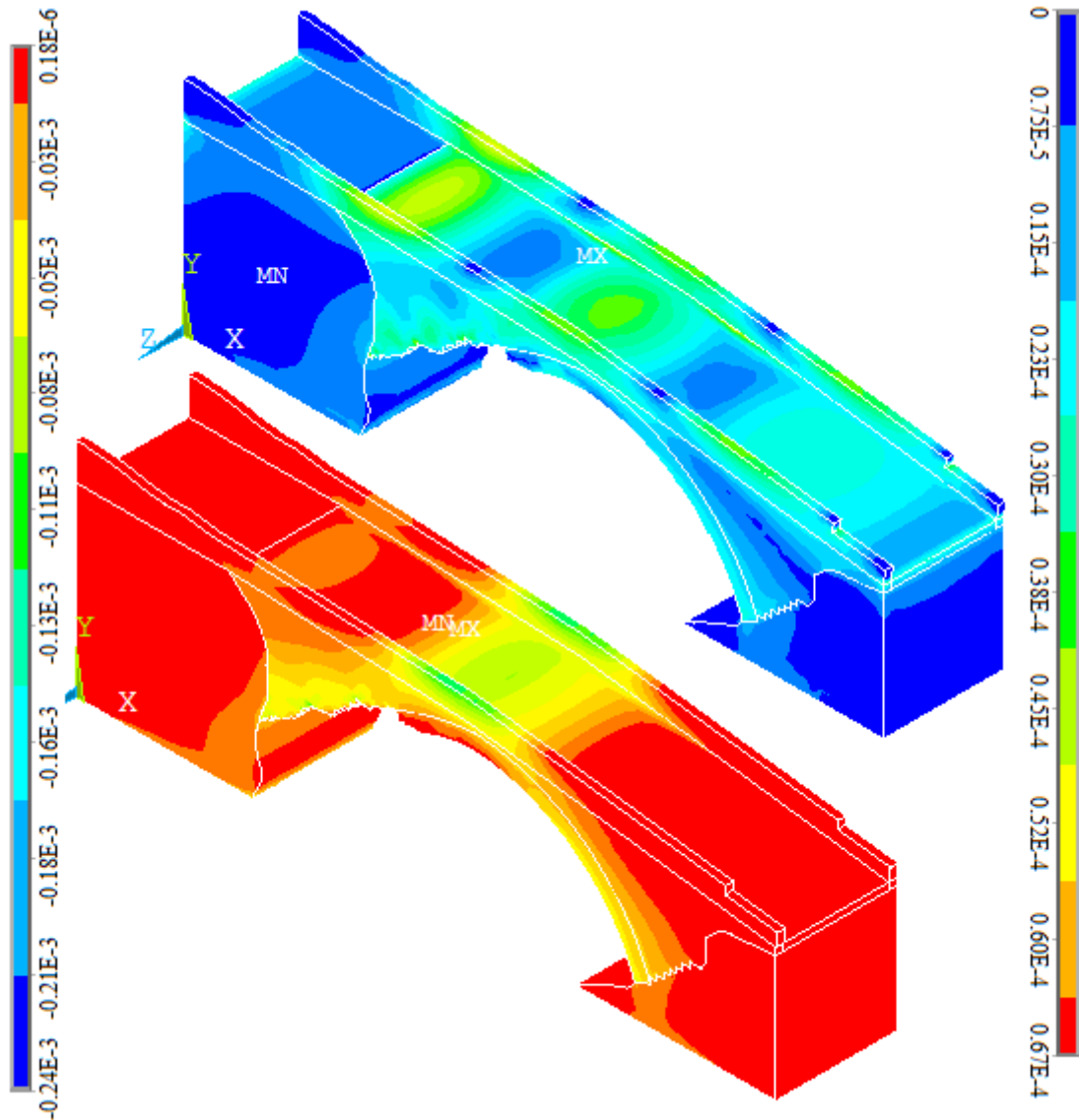


Fig. 8 Maximum and minimum elastic strains of the masonry bridge before restoration under dead load

4.1.2 Structural response under live load

Structural behavior of the masonry arch bridge is examined under dead and live loads in this part of the paper. The live load on the bridge is considered as 500 kg/m^2 for maximum human crowd. The maximum vertical displacements contour of the bridge before restorations under live load is shown in Fig. 9. It is seen that displacements decrease from the middle point of the bridge arch to side supports and foots. The maximum displacement occurs at the middle of the arch (damaged sections) as 1.63 mm.

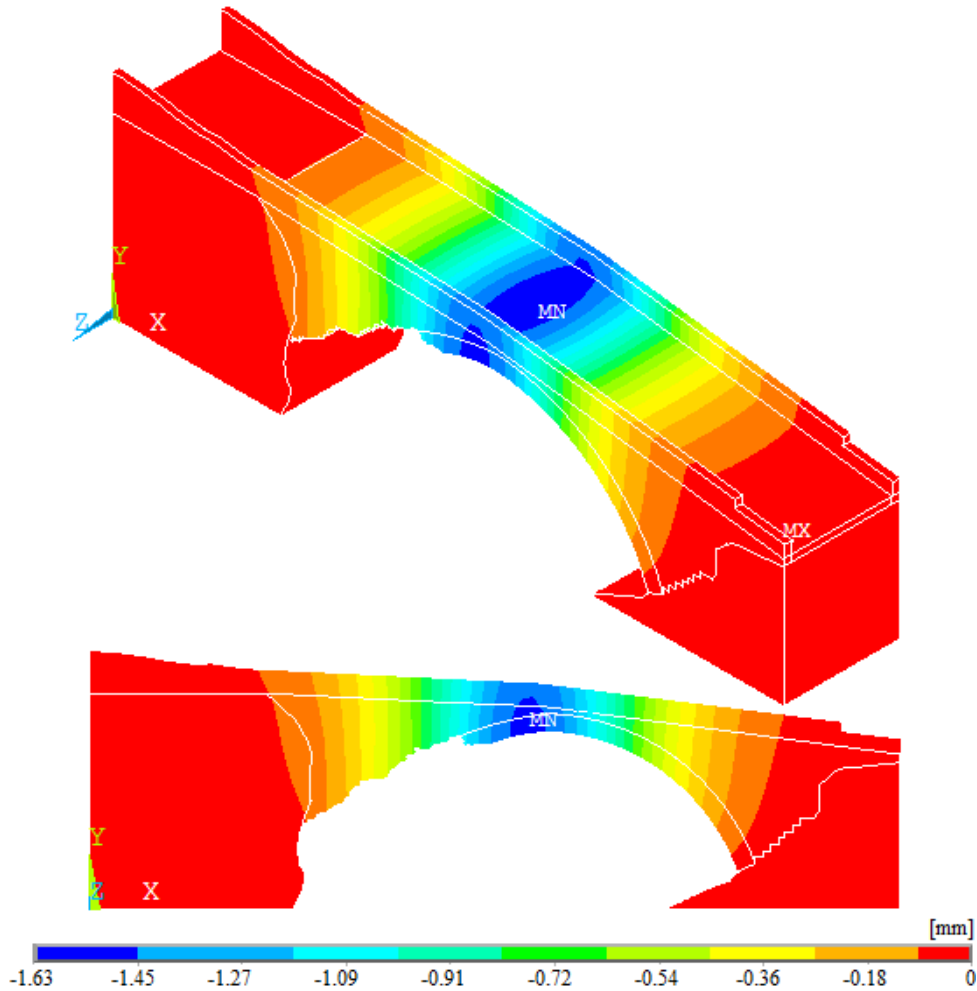


Fig. 9 Maximum displacement contours of the masonry bridge before restoration under live load

The maximum tensile stress contour of the bridge before restorations under live load is shown in Fig. 10. It is seen that maximum values of the tensile stresses consist on the contact points between bridge and side slopes as a 0.60 MPa, locally. Also, some stress accumulations regions are determined on the side walls, arches and parapets valued at 0.29 MPa. Excluding these sections, maximum tensile stresses are attained as 0.10 MPa.

The maximum compressive stress contour of the bridge before restorations under live load is shown in Fig. 11. It is seen that maximum values of the compressive stresses consist on the lower parts of the damaged side walls and arches as a 1.96MPa. Also, some stress accumulations regions are determined on the side walls and arches (especially right side of the arches and near of the supports) valued at 1.25 MPa. Excluding these sections, maximum compressive stresses are attained as 0.54 MPa.

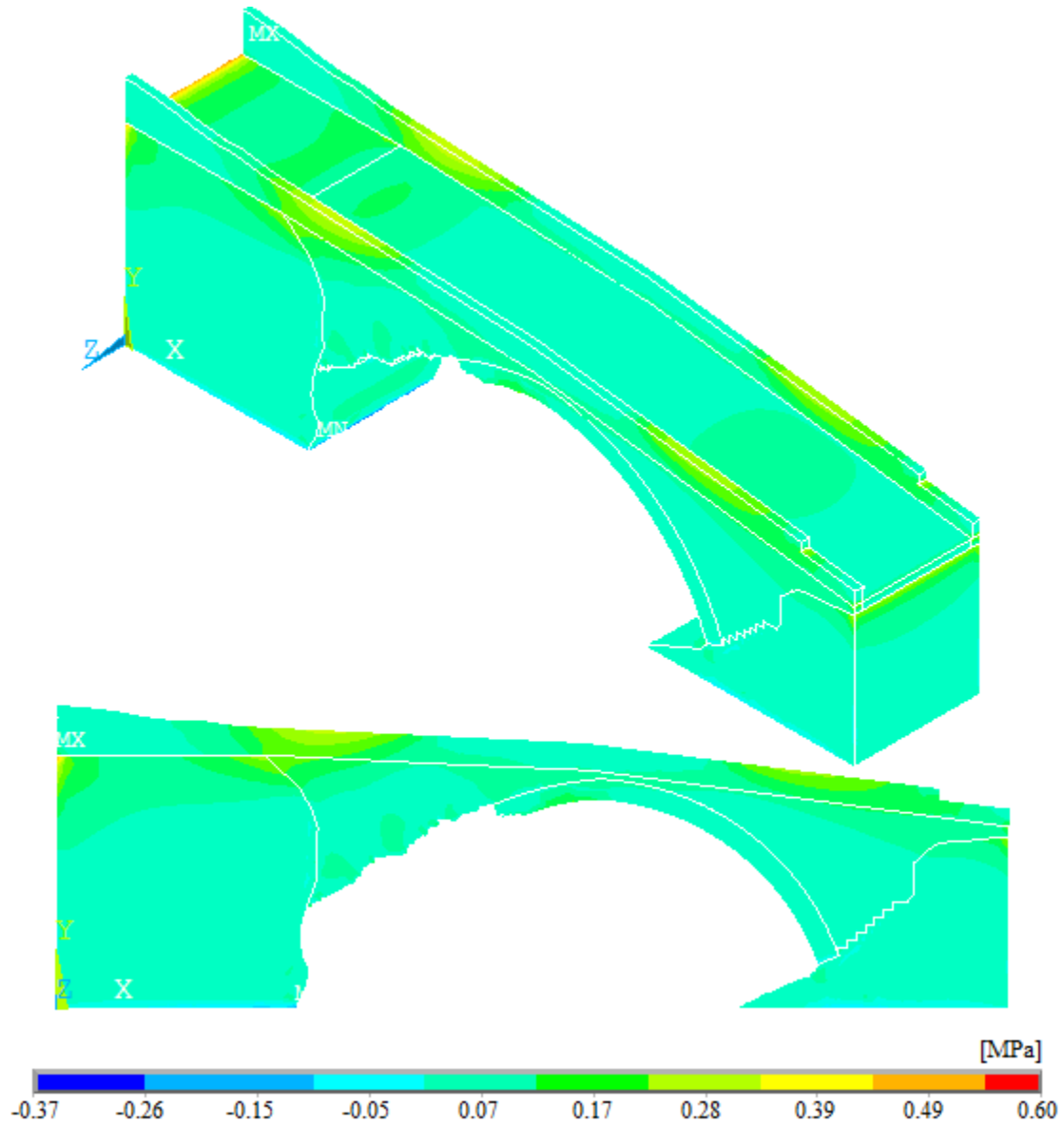


Fig. 10 Maximum tensile stress of the masonry bridge before restoration under live load

The maximum compressive stress contour of the bridge before restorations under live load is shown in Fig. 11. It is seen that maximum values of the compressive stresses consist on the lower parts of the damaged side walls and arches as a 1.96 MPa. Also, some stress accumulations regions are determined on the side walls and arches (especially right side of the arches and near of the supports) valued at 1.25 MPa. Excluding these sections, maximum compressive stresses are attained as 0.54 MPa.

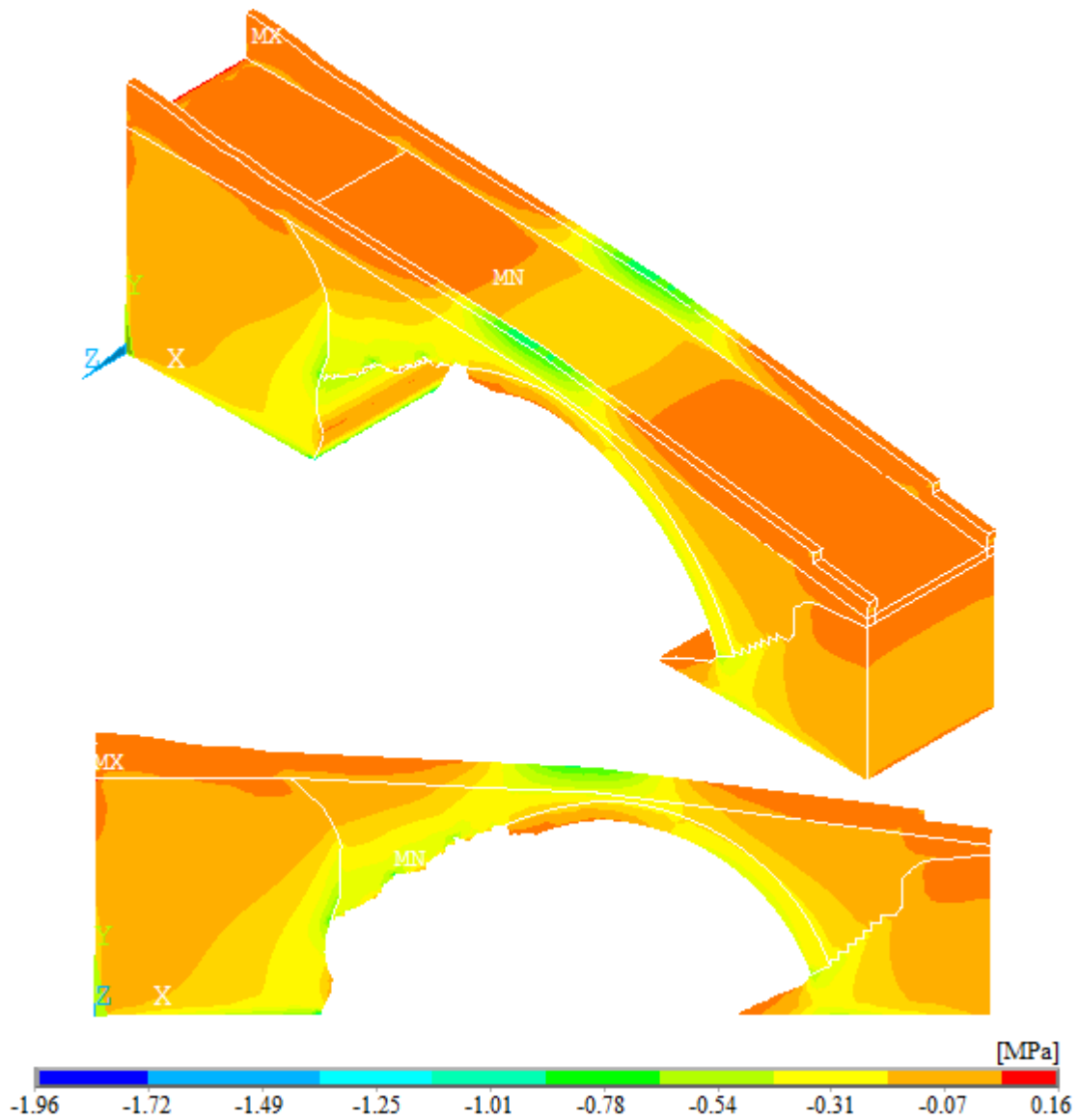


Fig. 11 Maximum compressive stress of the masonry bridge before restoration under live load

The maximum and minimum elastic strains contours of the bridge before restorations under live load are shown in Fig. 12. It is seen that maximum and minimum values of the elastic strains attained as $0.79\text{E-}4$ and $0.27\text{E-}3$, respectively. Also, some strain accumulations regions are determined for maximum elastic strains on the damaged side walls, lower and inner part of the arches, and some points on the roadway valued at $0.39\text{E-}4$. As well as, some strain accumulations regions are attained for minimum elastic strains on the inner part of the arches, some points of parapets and lower sections of side walls near the arch valued at $0.10\text{E-}3$.

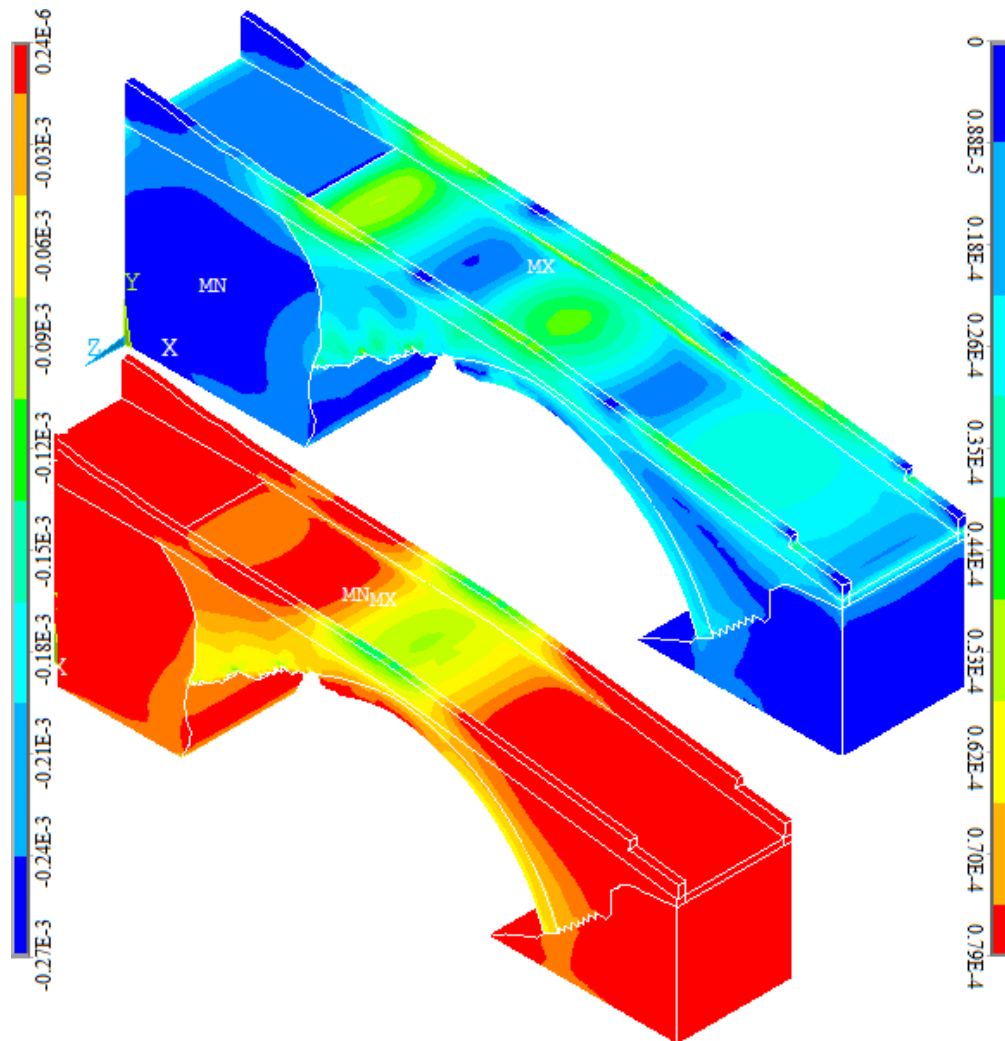


Fig. 12 Maximum and minimum elastic strains of the masonry bridge before restoration under live load

4.1.3 Structural response under dead load, live loads and dynamic (earthquake) loads

Earthquake behavior of Dandalaz masonry arch bridge before restoration is performed using is performed using ERZIKAN/ERZ-NS component of 1992 Erzincan earthquake ground motion (Fig. 13) [URL-1]. Because of the fact that the earthquake was occurred in our country, this ground motion record is used to obtain the more specific and reliable results. This record is applied to first mode direction obtained from the modal analyses of the bridge.

Element matrices are computed using the Gauss numerical integration technique (Bathe 1996). The Newmark method is used in the solution of the equation of motion. Rayleigh damping is considered in the analyses as 5%. Because of needed too much memory for the analyses, first 6.5 second of the ground motions, which is the most effective duration, is taken into account in calculations.

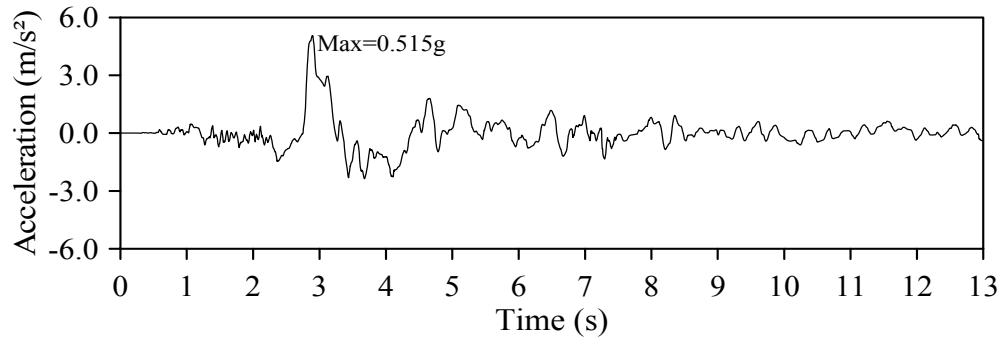


Fig. 13 The time-history of ground motion acceleration of 1992 Erzincan earthquake

The maximum vertical displacements contour of the bridge before restorations under dynamic loads is shown in Fig. 14. It is seen that displacements decrease from the middle point of the bridge arch to side supports and foots. The maximum displacement occurs at the middle of the arch (damaged sections) as 2.63 mm.

The maximum tensile stress contour of the bridge before restorations under dynamic loads is shown in Fig. 15. It is seen that maximum values of the tensile stresses consist on the contact points between bridge and side slopes as a 1.02 MPa, locally. Also, some stress accumulations regions are determined on the side walls, arches and parapets valued at 0.68 MPa. Excluding these sections, maximum tensile stresses are attained as 0.38 MPa.

The maximum compressive stress contour of the bridge before restorations under dynamic loads is shown in Fig. 16. It is seen that maximum values of the compressive stresses consist on the lower parts of the damaged side walls and arches as a 2.89 MPa. Also, some stress accumulations regions are determined on the side walls and arches (especially right side of the arches and near of the supports) valued at 1.99 MPa. Excluding these sections, maximum compressive stresses are attained as 0.84 MPa.

The maximum and minimum elastic strains contours of the bridge before restorations under dynamic loads are shown in Fig. 17. It is seen that maximum and minimum values of the elastic strains attained as $0.95E-4$ and $0.50E-3$, respectively. Also, some strain accumulations regions are determined for maximum and minimum elastic strains valued at $0.69E-4$ and $0.27E-3$, respectively.

4.2 Finite element analysis of the bridge after restoration

In the finite element model of the bridge after restoration, it has been adopted that damaged elements are completed and strengthened. Also, stone retaining walls and foundations given in restoration projects with detail are taken into account to reflect the structural behavior of the masonry bridge as soon as possible. 3D finite element model of the bridge constituted using ANSYS software shown in Fig. 18. In the finite element model, three dimensional solid elements have been used. This model consists of 138190 nodes and 94586 mesh elements. All analyses are performed as linear elastic. As boundary conditions, all of freedoms under the bridge abutments and at the side walls are considered as fixed. The material properties considered in the analysis of the bridge after restorations are given in Table 2.

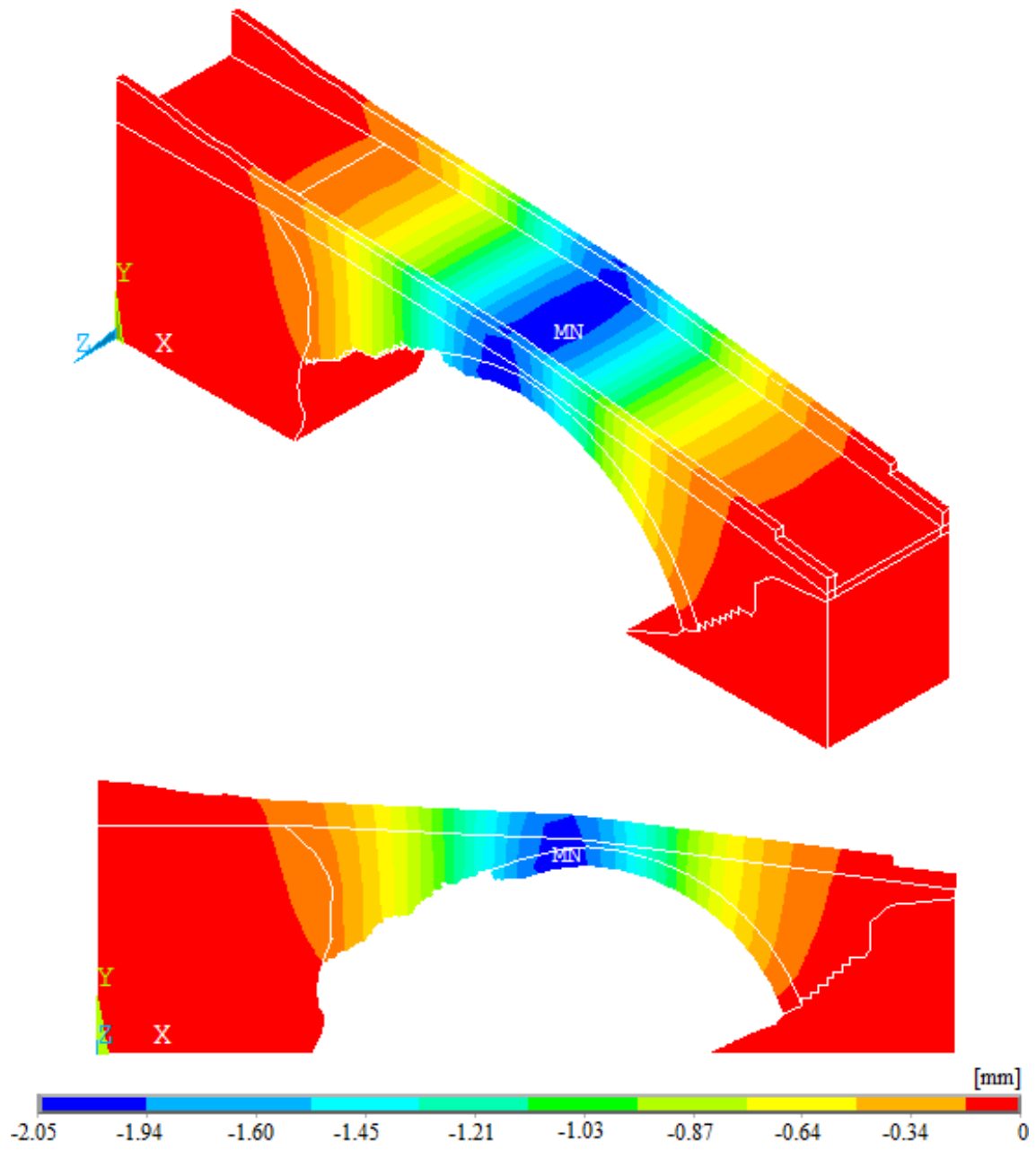


Fig. 14 Maximum displacement contours of the masonry bridge before restoration under dynamic loads

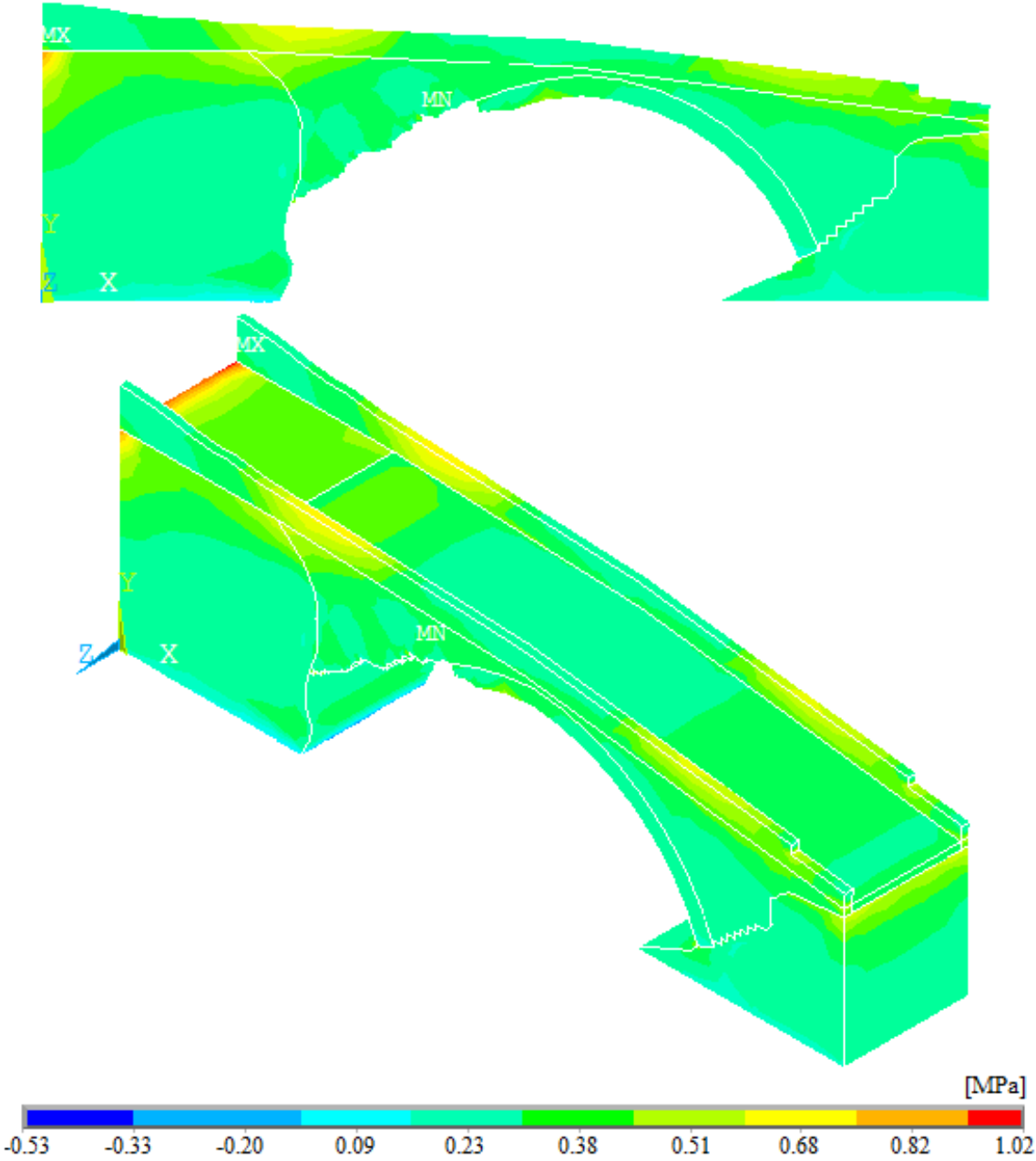


Fig. 15 Maximum tensile stress of the masonry bridge before restoration under dynamic loads

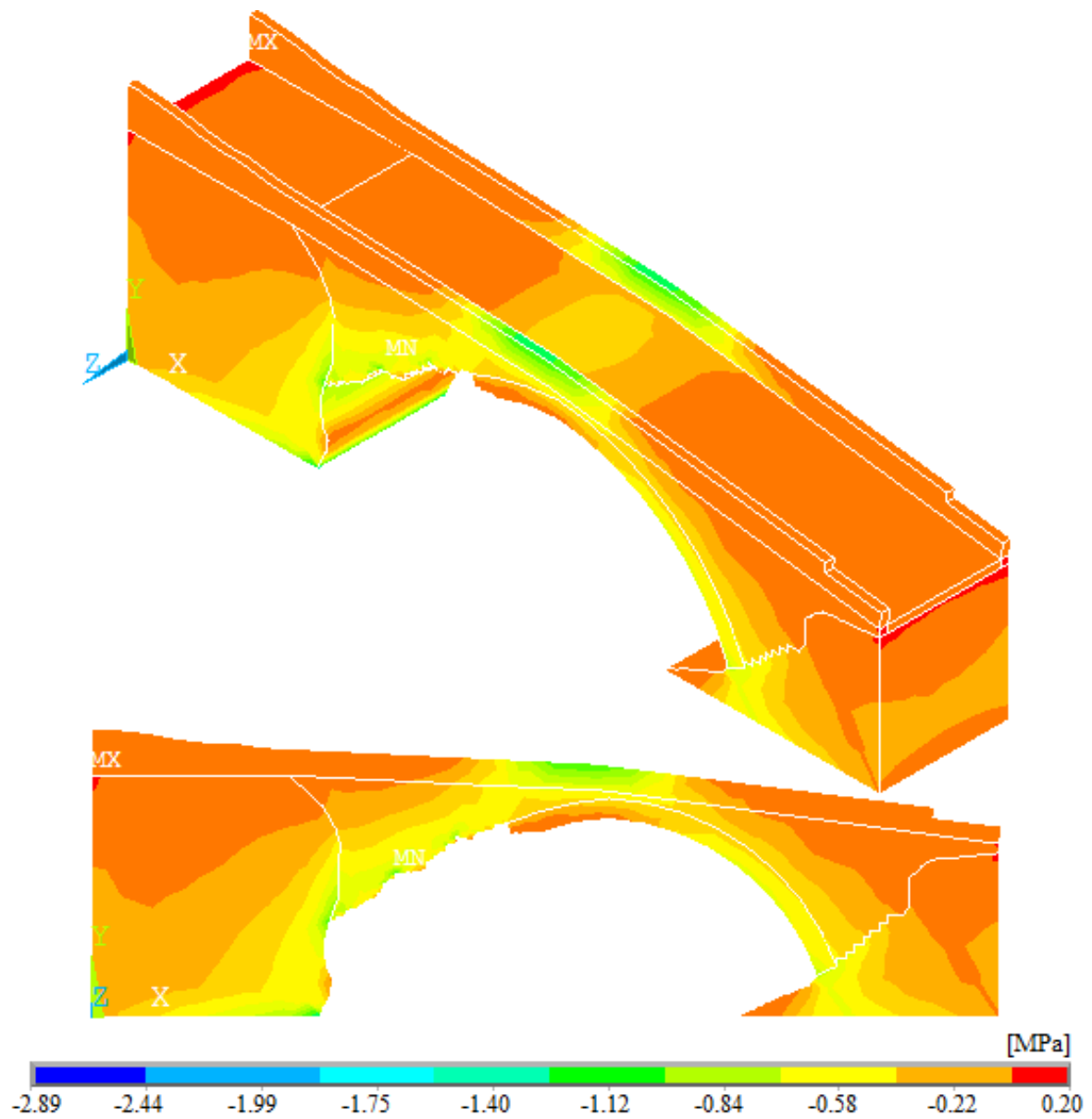


Fig. 16 Maximum compressive stress of the masonry bridge before restoration under dynamic loads

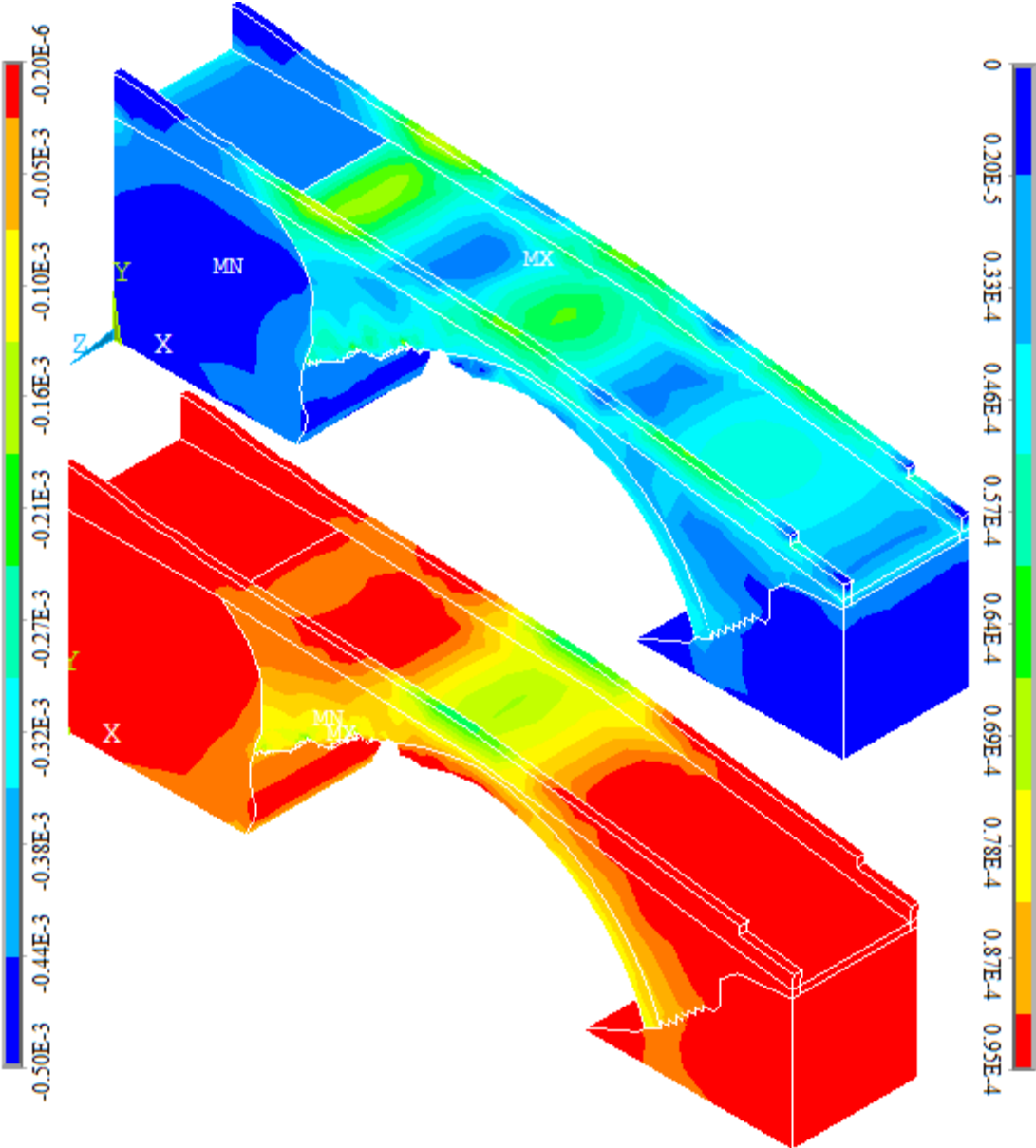


Fig. 17 Maximum and minimum elastic strains of the masonry bridge before restoration under dynamic loads

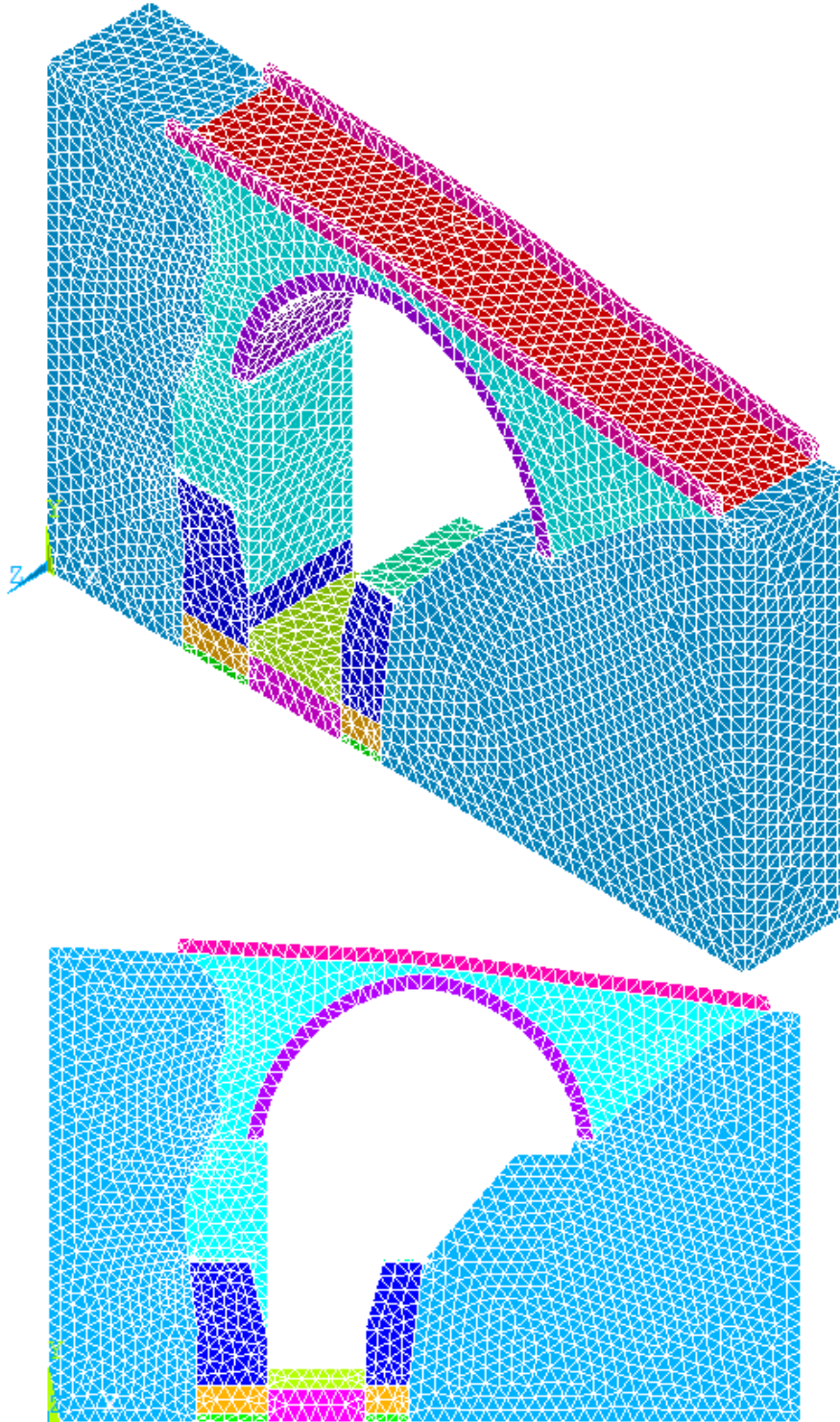


Fig. 18 Finite element model of Dandalaz masonry arch bridge after restoration

Table 2 Material properties considered in the analytical analysis after restorations

Structural Elements	Material Properties		
	Modulus of Elasticity (N/m^2)	Poisson Ratio (-)	Density (kg/m^3)
Arches	1.7E10	0.30	2000
Side Walls	1.7E10	0.30	2000
Timber Blocks	8.0E09	0.30	1200
Slope	2.0E10	0.35	2500
Parapets	1.7E10	0.30	2000
Foundations	2.0E10	0.20	2500
Concrete under foundation	2.0E10	0.20	2500
Ground	2.0E10	0.35	2500
Filling above ground	1.7E10	0.30	2000
Stone retaining walls	1.7E10	0.30	2000
Filling above stone retaining walls	1.7E10	0.30	2000

4.2.1 Structural response under dead load

The maximum vertical displacements contour of the bridge after restorations under dead load is shown in Fig. 19. It is seen that displacements decrease from the middle point of the bridge arch to side supports and foots. The maximum displacement occurs at the middle of the bridge arch as 0.46 mm. Also, it is seen that the distribution of the displacements in the structural elements continues more harmonious after restoration. This situation shows that the restoration has positive effect on system behavior.

The maximum tensile stress contour of the bridge after restorations under dead load is shown in Fig. 20. It is seen that maximum values of the tensile stresses consist on the contact points between bridge and side slopes as a 1.40 MPa, locally. Excluding these sections, maximum tensile stresses are attained as 0.49 MPa.

The maximum compressive stress contour of the bridge after restorations under dead load is shown in Fig. 21. It is seen that maximum values of the compressive stresses consist on the contact points between right-left sides of arch and slopes, cross sections of stone retaining walls with ground and support points as a 0.75 MPa. Excluding these sections, maximum compressive stresses are attained as 0.35 MPa.

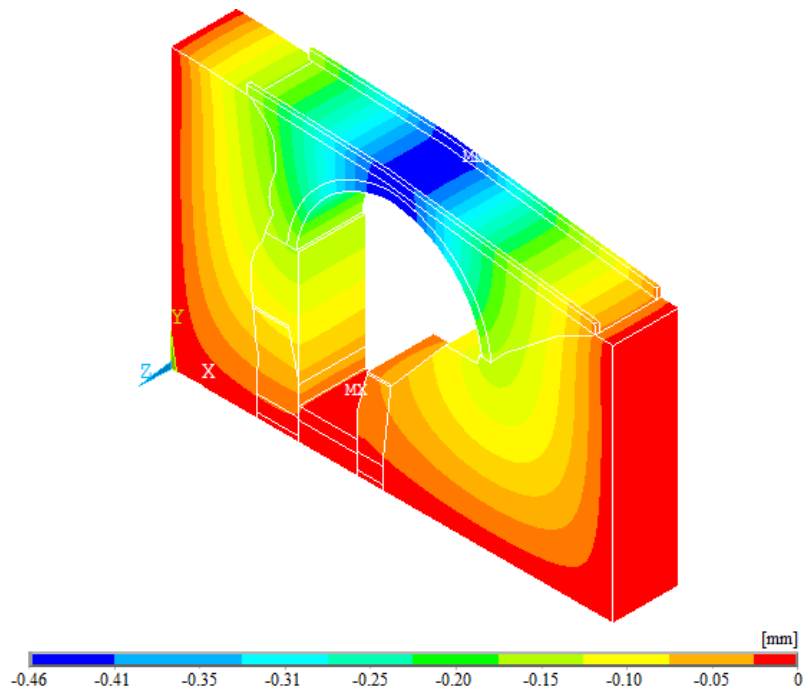


Fig. 19 Maximum displacement contours of the masonry bridge after restoration under dead load

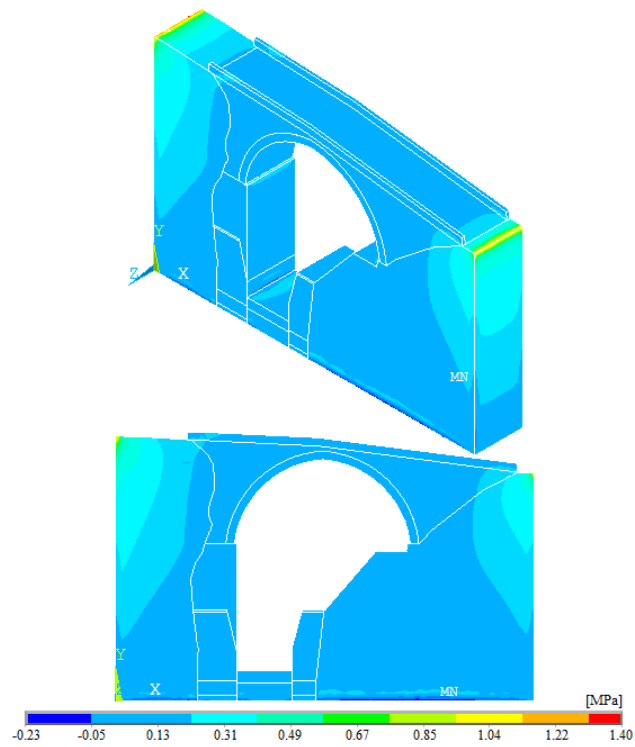


Fig. 20 Maximum tensile stress of the masonry bridge after restoration under dead load

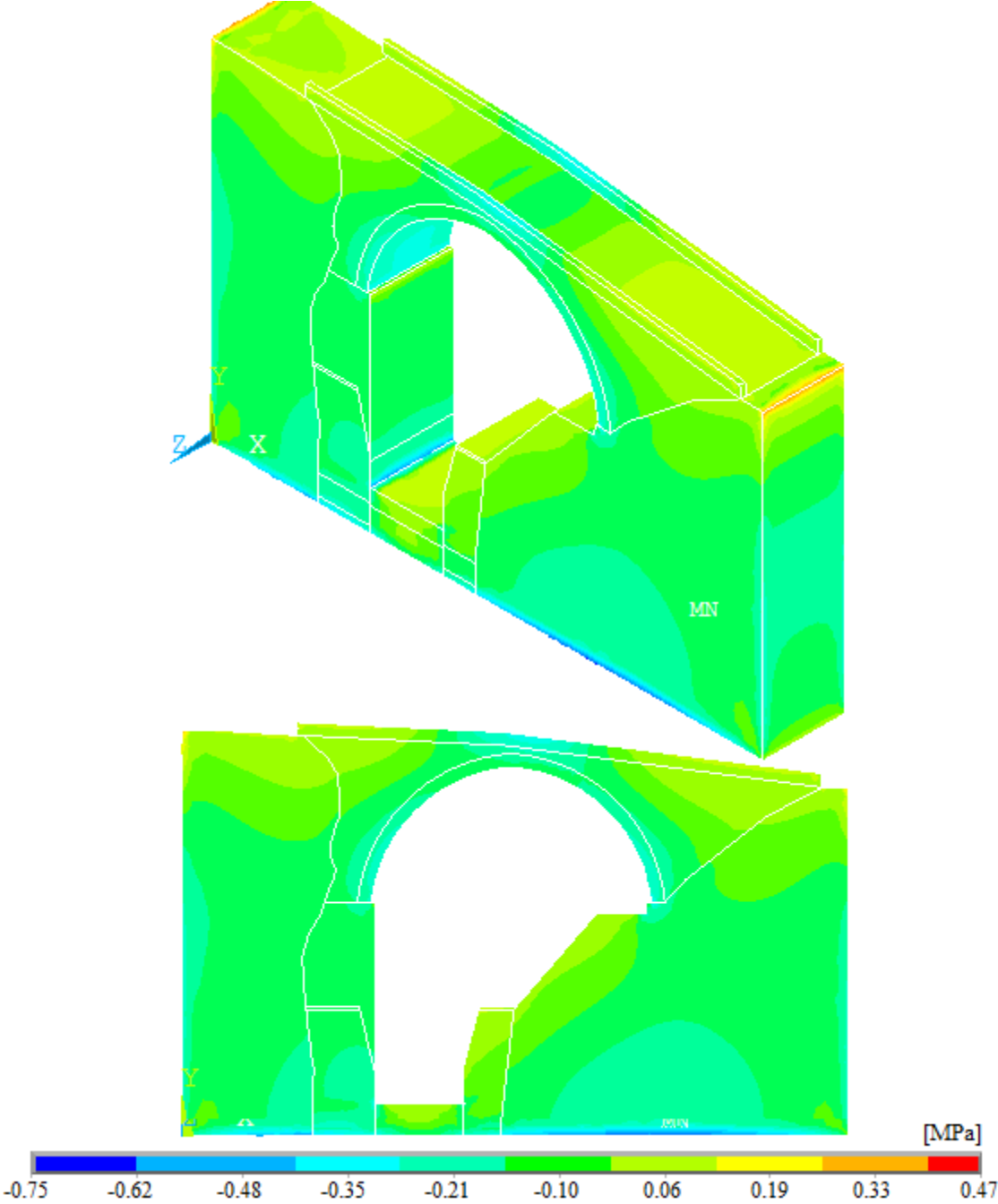
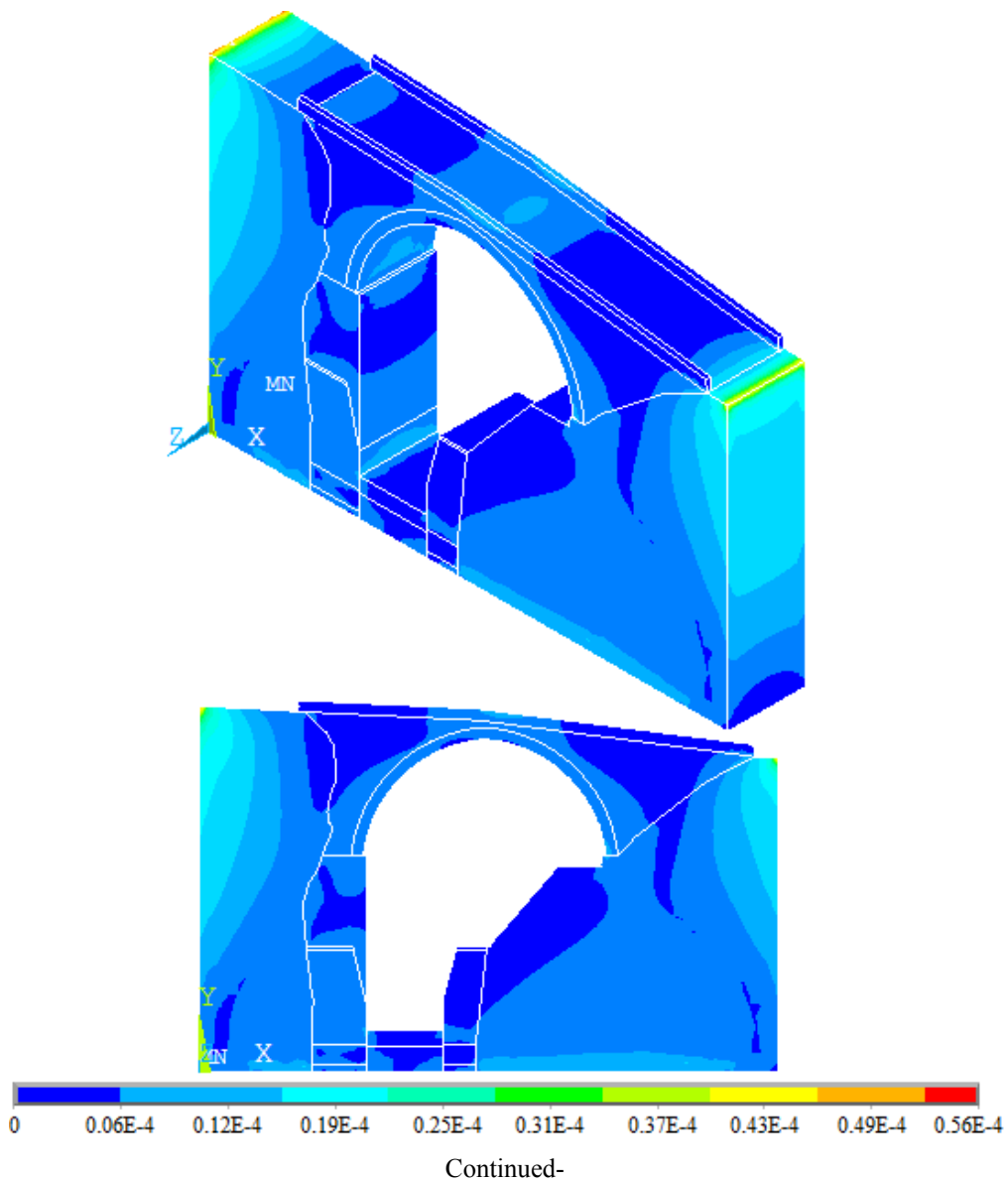


Fig. 21 Maximum of the compressive stress of the masonry bridge after restoration under dead load

The maximum and minimum elastic strains contours of the bridge after restorations under dead load are shown in Fig. 22. It is seen that maximum and minimum values of the elastic strains attained as $0.56E-4$ and $0.36E-4$, respectively. Also, some strain accumulations regions are determined for maximum elastic strains on the arch, stone retaining walls and ground valued at $0.25E-4$. As well as, some strain accumulations regions are attained for minimum elastic strains on the arch, side walls and transition lines between stone retaining walls and ground-foundation valued at $0.24E-4$.



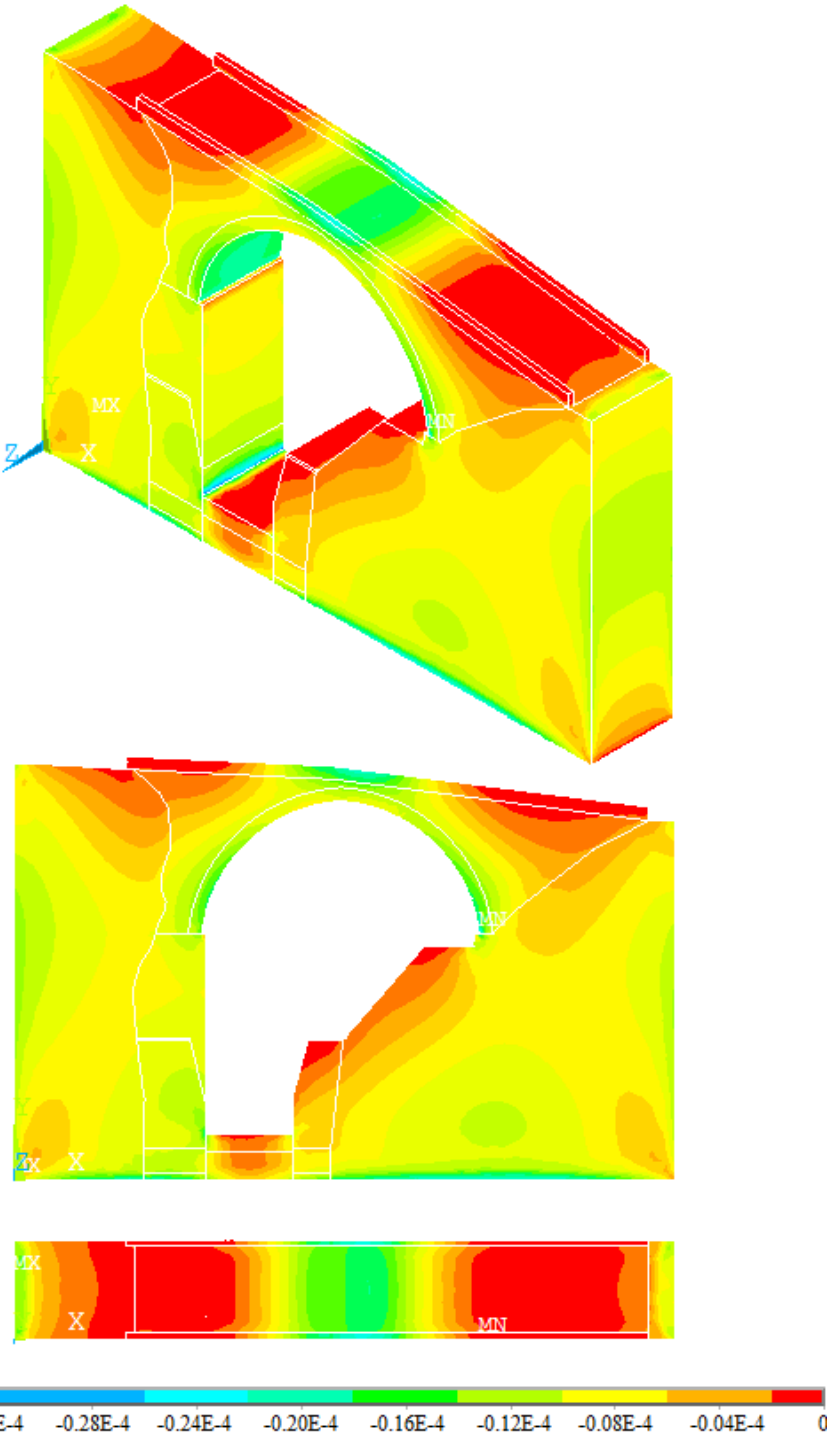


Fig. 22 Maximum and minimum elastic strains of the masonry bridge after restoration under dead load

4.2.2 Structural response under live load

Structural behavior of the masonry arch bridge is examined under dead and live loads in this part of the paper. The live load on the bridge is considered as 500 kg/m^2 for maximum human crowd. The maximum vertical displacements contour of the bridge after restorations under live load is shown in Fig. 23. It is seen that displacements decrease from the middle point of the bridge arch to side supports and foots. The maximum displacement occurs at the middle of the arch as 0.50 mm .

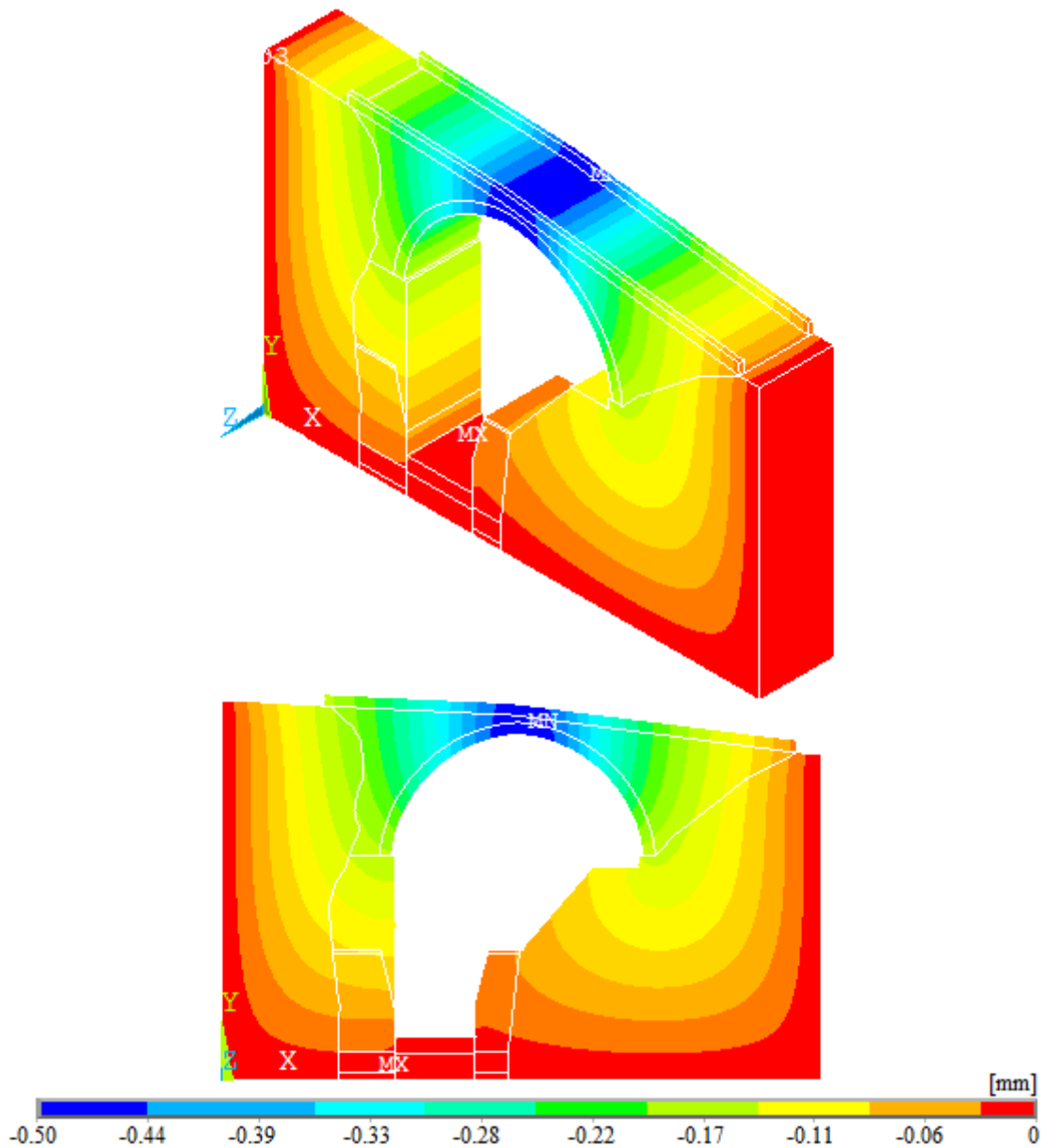


Fig. 23 Maximum displacement contours of the masonry bridge after restoration under live load

The maximum tensile stress contour of the bridge after restorations under live load is shown in Fig. 24. It is seen that maximum values of the tensile stresses consist on the contact points between bridge and side slopes as a 1.44 MPa, locally. Excluding these sections, maximum tensile stresses are attained as 0.51 MPa

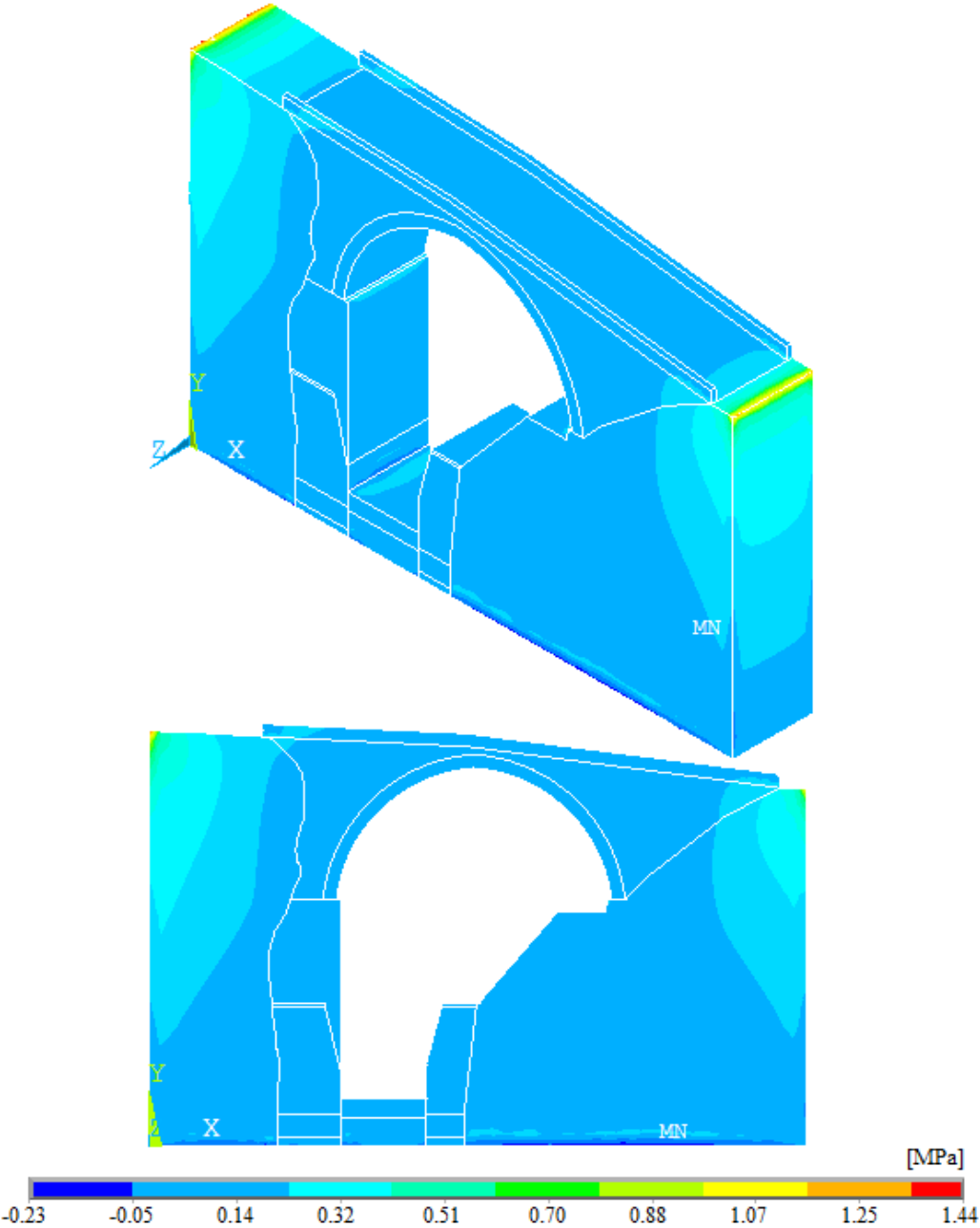


Fig. 24 Maximum tensile stress of the masonry bridge after restoration under live load

The maximum compressive stress contour of the bridge after restorations under live load is shown in Fig. 25. It is seen that maximum values of the compressive stresses consist on the interaction lines between right-left points of arch and ground, contact sections between stone retaining walls with slopes and ground, and under the foundation and supports as a 0.76 MPa. Excluding these sections, maximum compressive stresses are attained as 0.40 MPa.

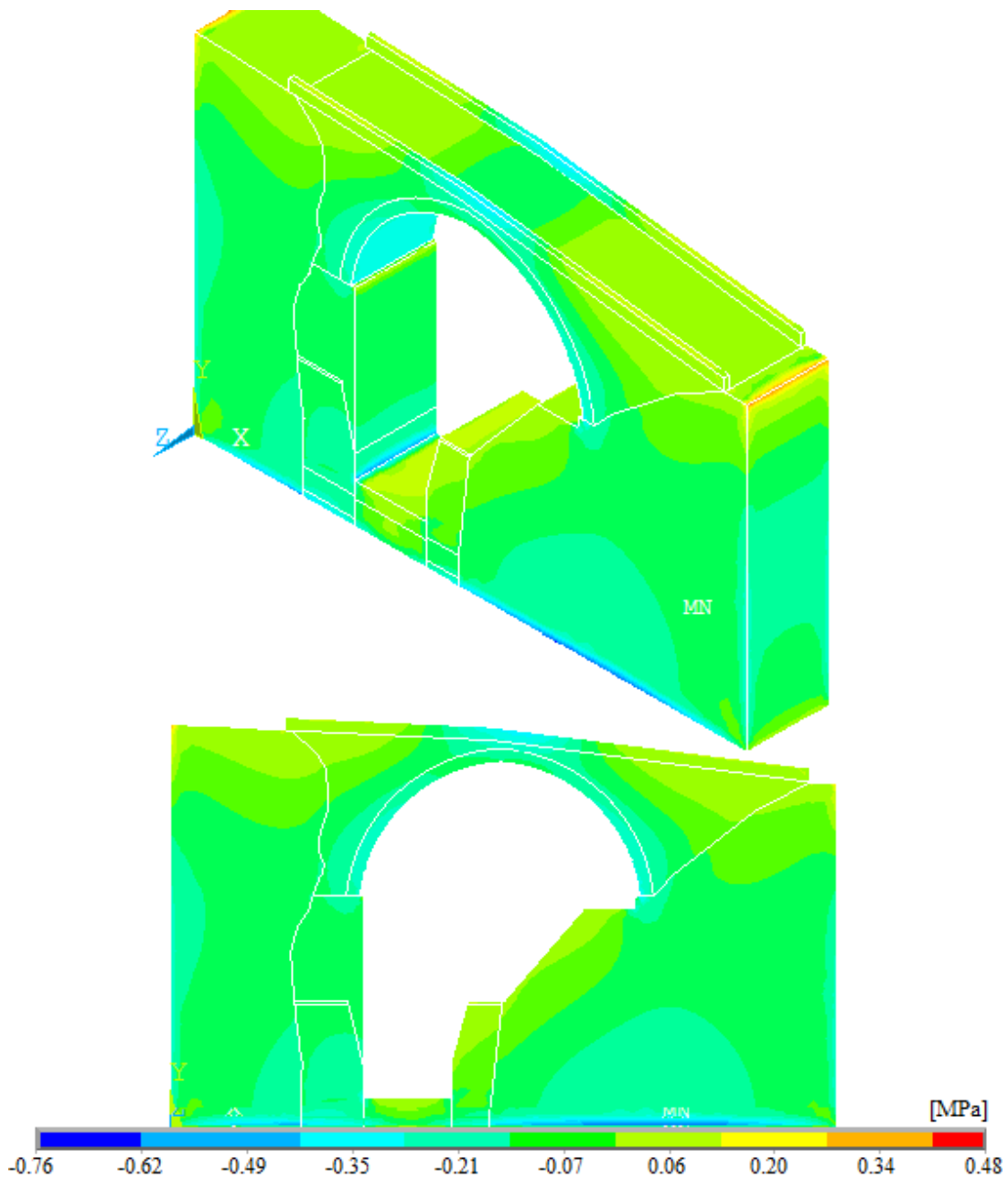
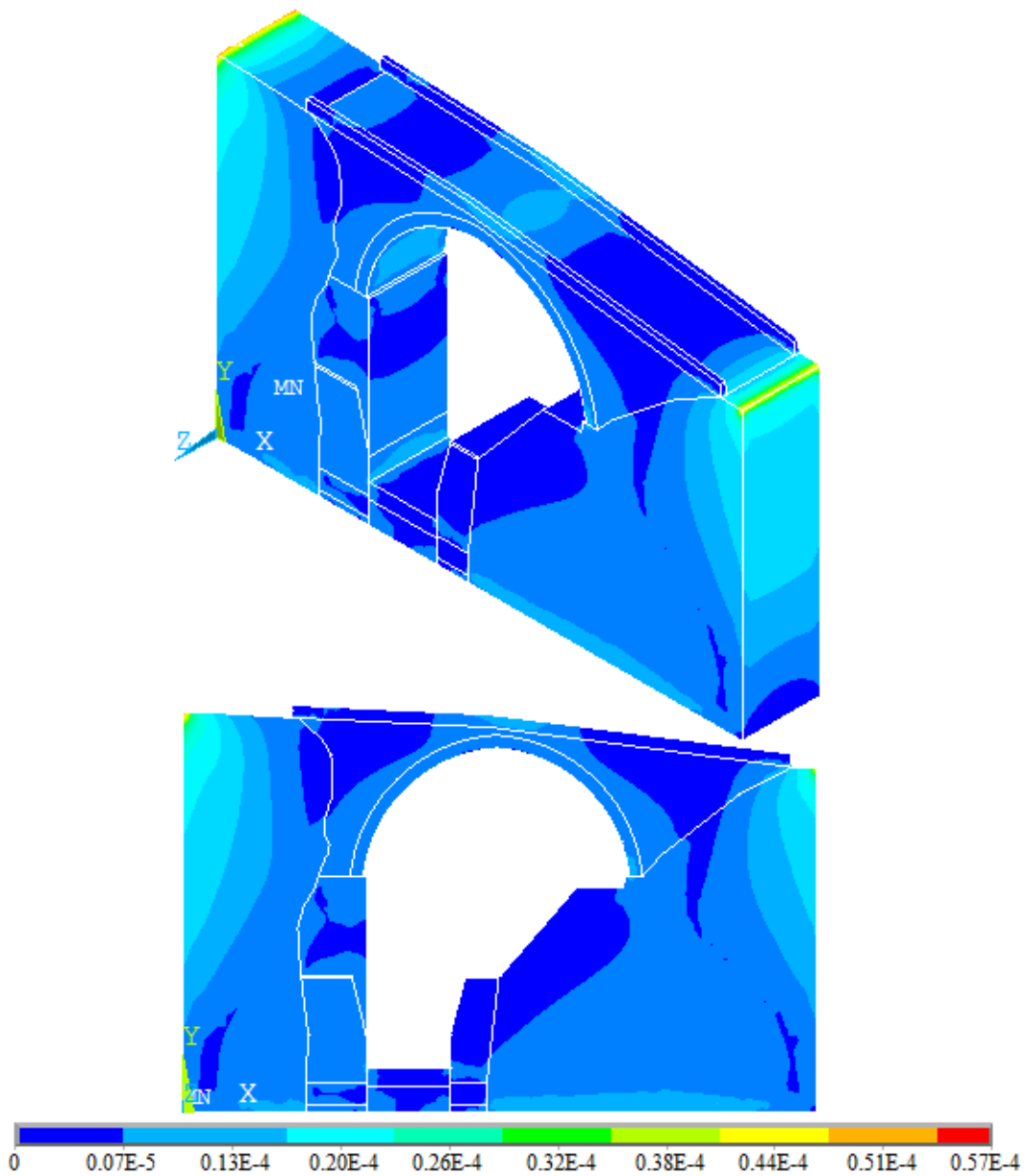


Fig. 25 Maximum compressive stress of the masonry bridge after restoration under live load

The maximum and minimum elastic strains contours of the bridge after restorations under live load are shown in Fig. 26. It is seen that maximum and minimum values of the elastic strains attained as $0.57E-4$ and $0.39E-4$, respectively. Also, some strain accumulations regions are determined for maximum elastic strains on the arch, stone retaining walls and ground valued at $0.26E-4$. As well as, some strain accumulations regions are attained for minimum elastic strains on the arch, side walls, roadway projection areas of the mid-span of the bridge arch and transition lines between stone retaining walls and ground-foundation valued at $0.26E-4$



Continued-

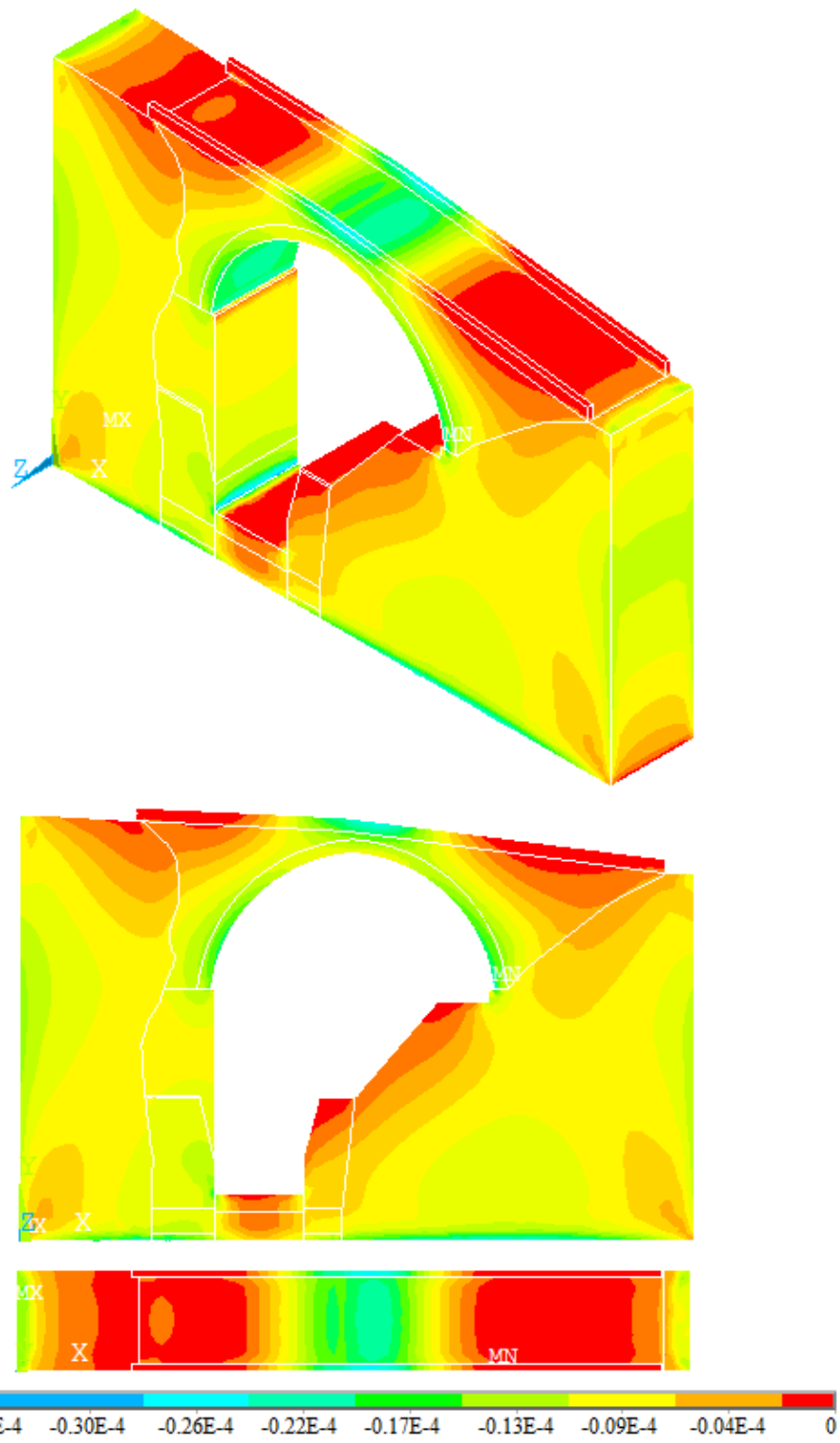


Fig. 26 Maximum and minimum elastic strains of the masonry bridge after restoration under live load

4.2.3 Structural response under dead load, live loads and dynamic (earthquake) loads

Earthquake behavior of Dandalaz masonry arch bridge after restoration is performed using ERZIKAN/ERZ-NS component of 1992 Erzincan earthquake ground motion. The maximum vertical displacements contour of the bridge after restorations under dynamic loads is shown in Fig. 27. It is seen that displacements decrease from the middle point of the bridge arch to side supports and foots. The maximum displacement occurs at the middle of the arch as 0.95 mm.

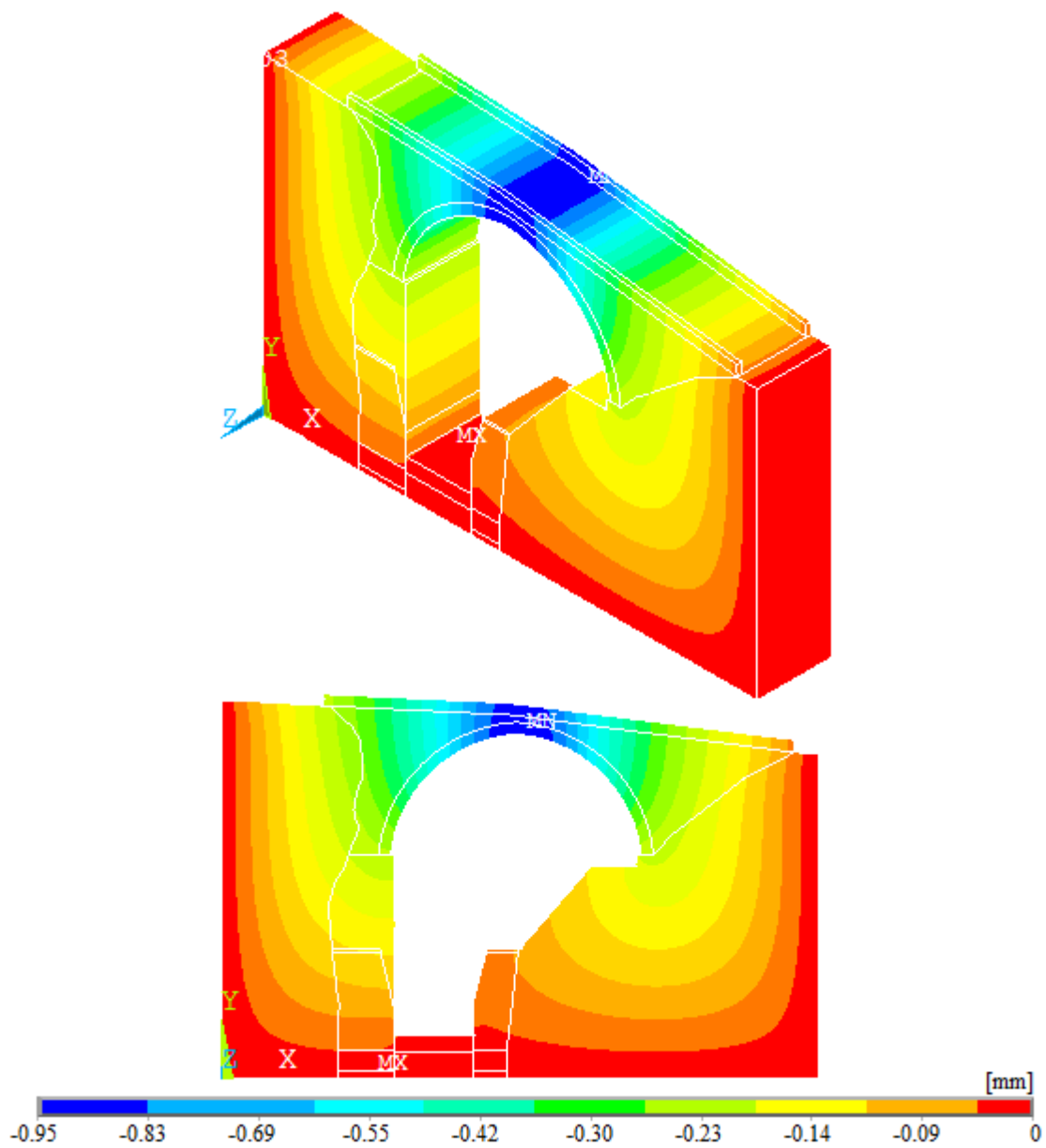


Fig. 27 Maximum displacement contours of the masonry bridge after restoration under dynamic loads

The maximum tensile stress contour of the bridge after restorations under dynamic loads is shown in Fig. 28. It is seen that maximum values of the tensile stresses consist on the contact points between bridge and side slopes as a 1.65 MPa, locally. Excluding these sections, maximum tensile stresses are attained as 0.66 MPa.

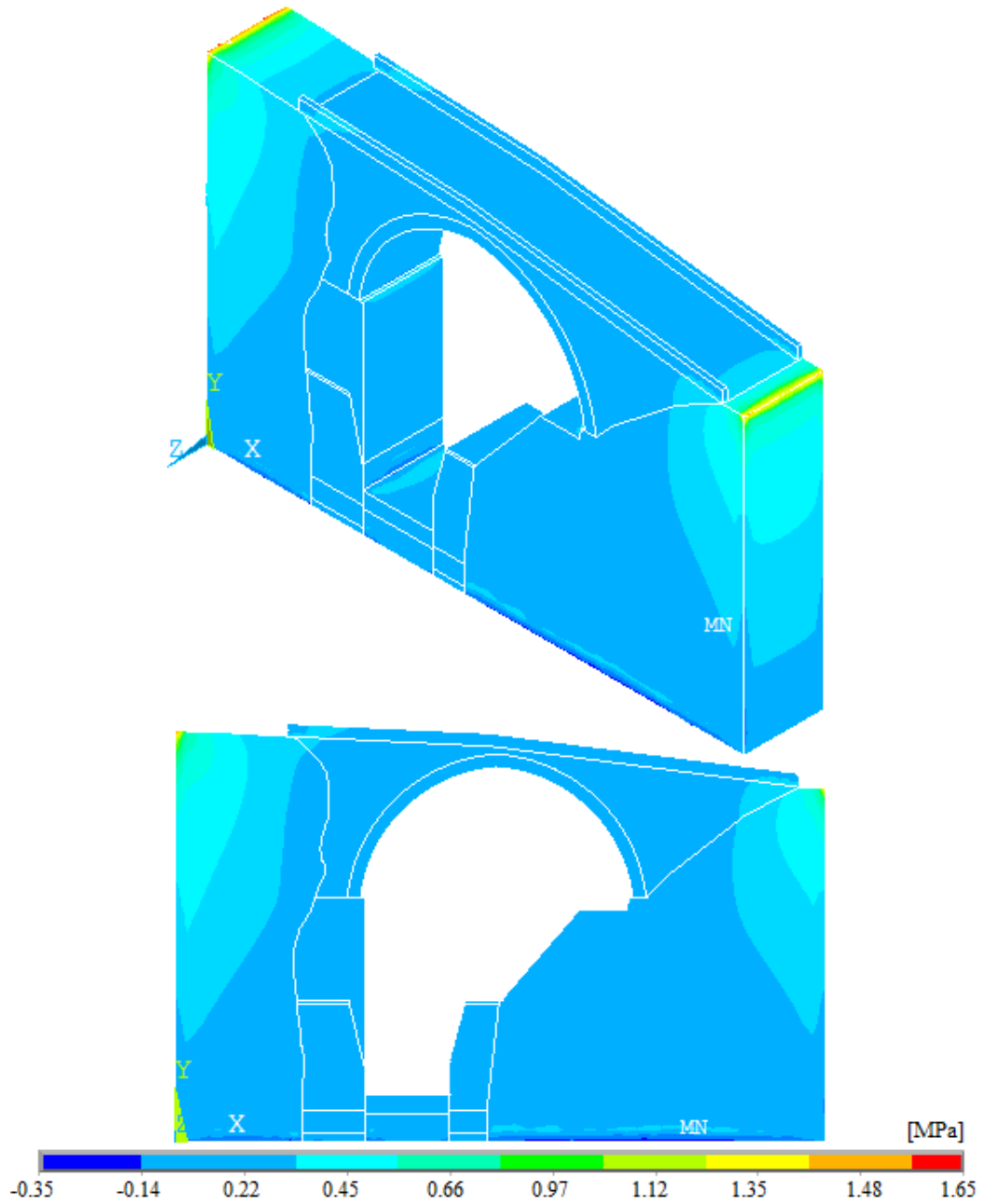


Fig. 28 Maximum tensile stress of the masonry bridge after restoration under dynamic loads

The maximum compressive stress contour of the bridge after restorations under dynamic loads is shown in Fig. 29. It is seen that maximum values of the compressive stresses consist on the side walls, arches (right side of the arches and near of the supports), contact sections between stone retaining walls with slopes and ground valued at 1.35 MPa. Excluding these sections, maximum compressive stresses are attained as 0.76 MPa.

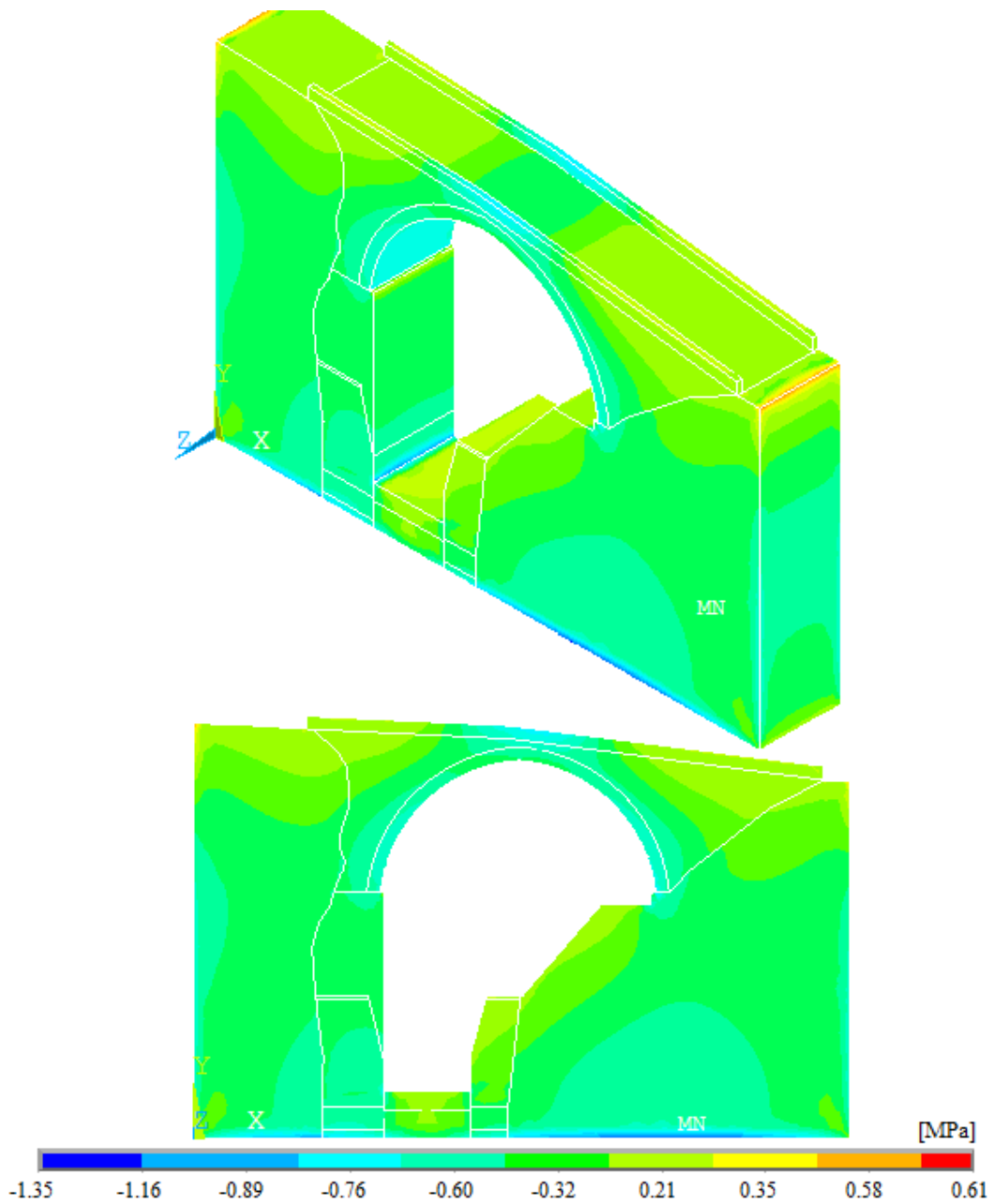
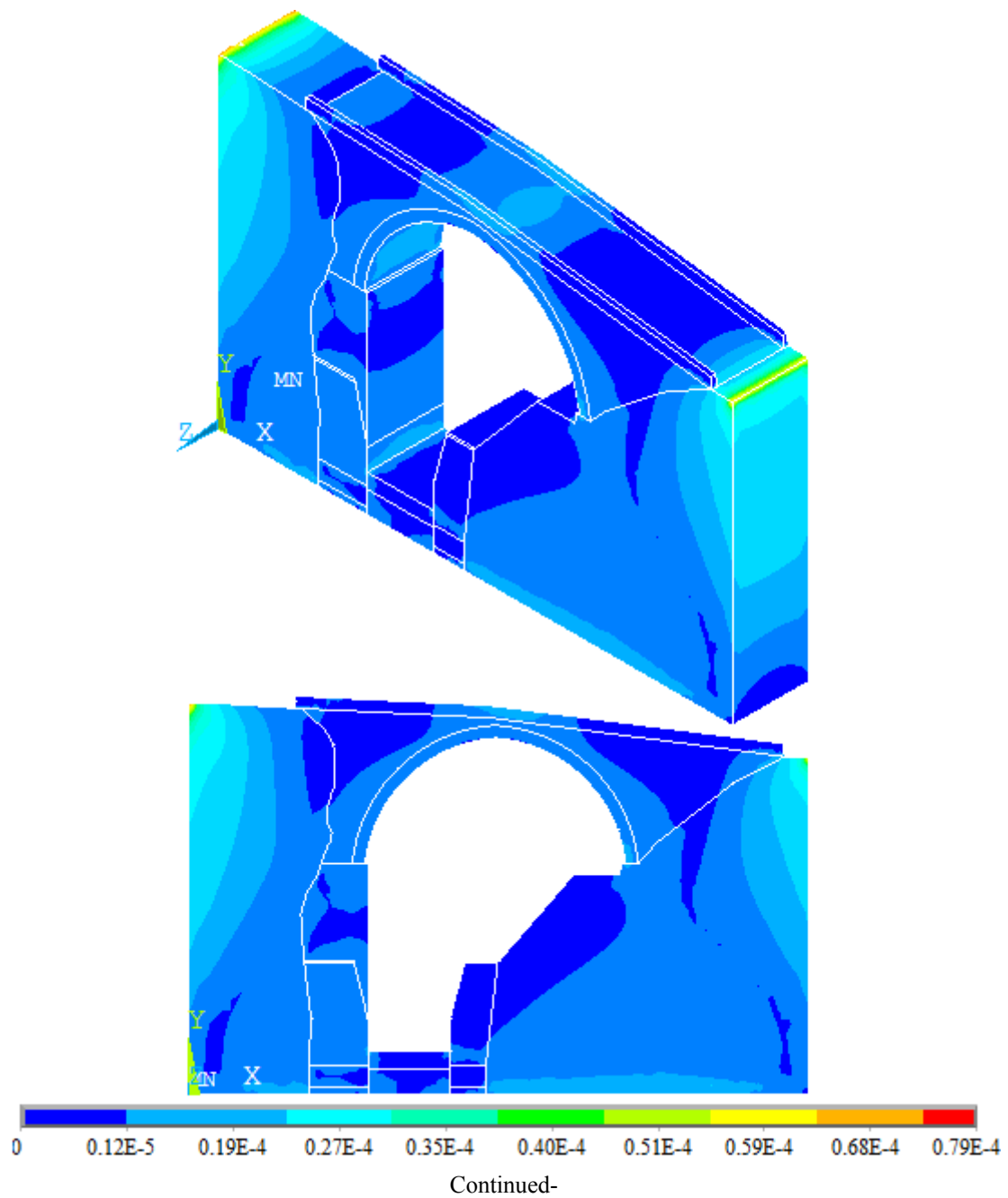


Fig. 29 Maximum compressive stress of the masonry bridge after restoration under dynamic loads

The maximum and minimum elastic strains contours of the bridge after restorations under dynamic loads are shown in Fig. 30. It is seen that maximum and minimum values of the elastic strains attained as $0.79E-4$ and $0.60E-4$, respectively. Also, some strain accumulations regions are determined for maximum and minimum elastic strains valued at $0.35E-4$ and $0.42E-4$, respectively.



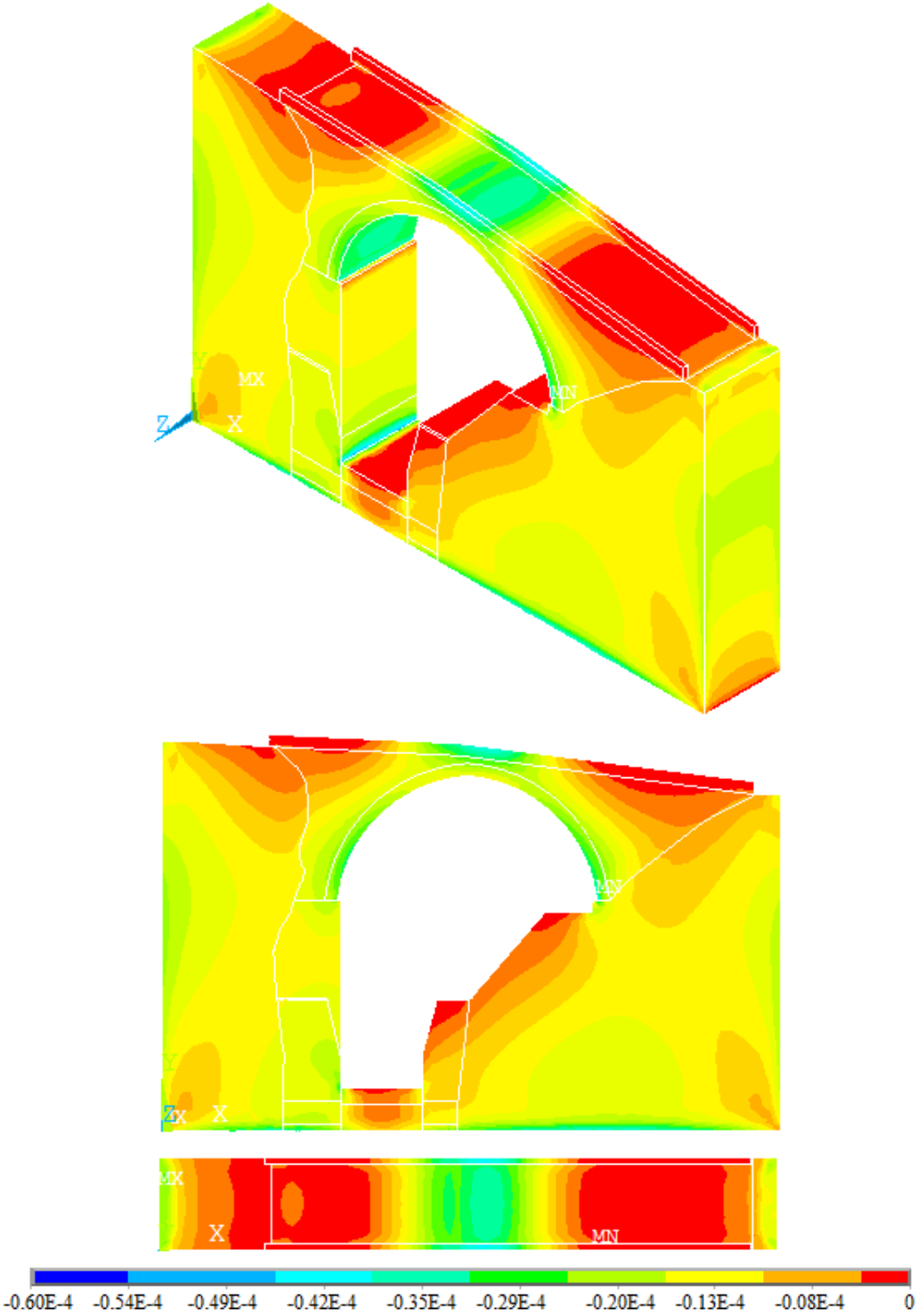


Fig. 30 Maximum and minimum elastic strains of the masonry bridge after restoration under dynamic loads

Table 3 Displacements, stresses and strains obtained from before restoration of the bridge

Analyses Results	Analyses Cases			
	Before Restoration			
	DL^*	DL^*+LL^*	$DL^*+LL^*+DYL^*$	
Displacements	1.40 mm	1.63 mm	2.05 mm	
Stresses	Tensile	0.58 MPa	0.60 MPa	1.02 MPa
		0.28 MPa	0.29 MPa	0.68 MPa
	Compressive	1.70 MPa	1.96 MPa	2.89 MPa
		1.08 MPa	1.25 MPa	1.99 MPa
Strains	Tensile	0.67E-4	0.79E-4	0.95E-4
		0.30E-4	0.39E-4	0.69E-4
	Compressive	0.24E-3	0.27E-3	0.50E-3
		0.08E-3	0.10E-3	0.27E-3
*DL: Dead load	*LL: Live Load	*DYL: Dynamic load		

Table 4 Displacements, stresses and strains obtained from after restoration of the bridge

Analyses Results	Analyses Cases			
	Before Restoration			
	DL^*	DL^*+LL^*	$DL^*+LL^*+DYL^*$	
Displacements	0.46 mm	0.50 mm	0.95 mm	
Stresses	Tensile	1.40 MPa	1.44 MPa	1.65 MPa
		0.49 MPa	0.51 MPa	0.66 MPa
	Compressive	0.75 MPa	0.76 MPa	1.35 MPa
		0.35 MPa	0.40 MPa	0.76 MPa
Strains	Tensile	0.56E-4	0.57E-4	0.79E-4
		0.25E-4	0.26E-4	0.35E-4
	Compressive	0.36E-4	0.39E-4	0.60E-4
		0.24E-4	0.26E-4	0.42E-4
*DL: Dead load	*LL: Live Load	*DYL: Dynamic load		

The analyses results obtained from before and after restoration of masonry arch bridge are summarized in Tables 3 and 4. The bold characters are used to imply the peak values which are obtained at the local points and may not be display the real behavior. The normal characters under the bold fonts are used to imply the general distributions of displacements, stresses and strains on the bridge. It is thought that these values can be used to compare the results with limit boundaries.

5. Conclusions

The objective of this study is to investigate the restoration effects on the structural behavior of masonry arch bridges. Dandalaz masonry arch bridge is chosen as an application. In the content of the paper, firstly finite element model of the bridge is constituted to reflect the current situation using building survey drawings. After, restoration project is explained and finite element model is reconstituted after restoration to compare the analyses results. For both conditions, maximum displacements, maximum-minimum principal stresses and maximum-minimum elastic strains are given with detail using contours diagrams and compared with each other to determine the restoration effects. Comparing the results of this study, the following observations can be made:

- *Analyses Results Before Restoration*

- ❖ In the finite element model of the bridge under current situation (before restoration), damaged elements are taken into account.
- ❖ The maximum displacement occurs at the middle of the arch (damaged sections) as 1.40 mm, 1.63 mm and 2.05 mm for dead load, live load and dynamic loads, respectively.
- ❖ Maximum values of the tensile stresses consist locally on the contact points between bridge and side slopes as a 0.58 MPa, 0.60 MPa and 1.02 MPa for dead load, live load and dynamic loads, respectively. Also, some stress accumulations regions are determined valued at 0.28 MPa, 0.29 MPa and 0.68 MPa for dead load, live load and dynamic loads, respectively.
- ❖ Maximum values of the compressive stresses consist locally on the lower parts of the damaged side walls and arches as a 1.70 MPa, 1.96 MPa and 2.89 MPa for dead load, live load and dynamic loads, respectively. Also, some stress accumulations regions are determined valued at 1.08 MPa, 1.25 MPa and 1.99 MPa for dead load, live load and dynamic loads, respectively.
- ❖ Maximum and minimum values of the elastic strains attained as 0.67E-4 and 0.24E-3, 0.79E-4 and 0.27E-3, 0.95E-4 and 0.50E-3 for dead load, live load and dynamic loads, respectively.

- *Analyses Results After Restoration*

- ❖ In the finite element model of the bridge after restoration, it has been adopted that damaged elements are completed and strengthened. Also, stone retaining walls and foundations given in restoration projects with detail are taken into account to reflect the structural behavior of the masonry bridge as soon as possible.
- ❖ The maximum displacement occurs at the middle of the arch as 0.46 mm, 0.50 mm and 0.95mm for dead load, live load and dynamic loads, respectively.

- ❖ Maximum values of the tensile stresses consist locally on the contact points between bridge and side slopes as a 1.40 MPa, 1.44 MPa and 1.65 MPa for dead load, live load and dynamic loads, respectively. Also, some stress accumulations regions are determined valued at 0.49 MPa, 0.51 MPa and 0.66 MPa for dead load, live load and dynamic loads, respectively.
- ❖ Maximum values of the compressive stresses consist locally on the contact points between right-left sides of arch and slopes, cross sections of stone retaining walls with ground and support points as a 0.75 MPa, 0.76 MPa and 1.35 MPa for dead load, live load and dynamic loads, respectively. Also, some stress accumulations regions are determined valued at 0.35 MPa, 0.40 MPa and 0.76 MPa for dead load, live load and dynamic loads, respectively.
- ❖ Maximum and minimum values of the elastic strains attained as 0.56E-4 and 0.36E-4, 0.57E-4 and 0.39E-4, 0.79E-4 and 0.60E-4 for dead load, live load and dynamic loads, respectively.

To determine the mechanical properties of materials used in the bridge, stone and mortar samples taken from the bridge are tested in the laboratory. As a result of the experimental studies, the compressive strength and weight per unit volume are determined as 50MPa and 2200-2400 kg/m³ for stones, respectively. Also, the compressive strength of the mortar is defined as 5-7MPa.

From the study, it can be seen that the restoration projects and studies have important and positive effects on the structural response of the bridge to transfer these structures to future.

References

- ANSYS (2008), Swanson Analysis System. U.S.A.
- Bathe, K.J. (1996), *Finite Element Procedures in Engineering Analysis*, Englewood Cliffs, New Jersey: Prentice-Hall.
- Bayraktar, A., Altunışık, A.C., Türker, T. and Sevim, B. (2007), "The model Updating of historical masonry bridges using operational modal analysis method", *Proceedings of the 1st Reinforcement and Transfer into the Future of Historical Structures*, Ankara, Turkey.
- Bayraktar, A., Türker, T., Sevim, B., Altunışık, A.C. and Yıldırım, F. (2009a), "Modal parameter identification of Hagia Sophia Bell-Tower via ambient vibration test", *J. Nondestruct. Eval.*, **28**(1), 37-47.
- Bayraktar, A., Birinci, F., Altunışık, A.C., Türker, T. and Sevim, B. (2009b), "Finite element model updating of Senyuva Historical Arch Bridge using ambient vibration tests", *The Baltic J. Road Bridge Eng.*, **4**(4), 177-185.
- Betti, M., Drosopoulos, G.A. and Stavroulakis, G.E. (2007), "On the collapse analysis of single span masonry/stone arch bridges with fill interaction", *Proceedings of the 5th International Conference on Arch Bridges*, ARCH'07, 617-624, Portugal.
- Brencich, A. and Sabia, D. (2008), "Experimental identification of a multi-span masonry bridge: The Tanaro Bridge", *Constr. Build. Mater.*, **22**, 2087-2099.
- Frunzio, G., Monaco, M. and Gesualdo, A. (2001), "3D FEM analysis of a Roman Arch Bridge", *Historical Constr.*, 591-598.
- Gonen, H., Dogan, M., Karacasu, M., Ozbasaran, H. and Gokdemir, H. (2013), "Structural failures in retrofit historical masonry arch bridge", *Eng. Fail. Anal.*, **35**, 334-342.
- Leon, J. and Espejo, S.R. (2007), "Load test to collapse on the masonry arch bridge at Urnieta", *Proceedings of the 5th International Conference on Arch Bridges*, ARCH'07, 969-977, Portugal.
- Milani, G. and Lourenço, P.B. (2012), "3D non-linear behavior of masonry arch bridges", *Comput. Struct.*, **110-111**, 133-150.

- Paegliti, A. and Paeglitis, A. (2009), "Restoration of masonry arch bridge over Venta River in Kuldiga", *Proceedings of the Starptautiska Baltijas Ceļu Conference*, 24-26 August, Latvia.
- Pela, L., Aprile, A. and Benedetti, A. (2013), "Comparison of seismic assessment procedures for masonry arch bridges", *Constr. Build. Mater.*, **38**, 381-394.
- Reccia, E., Milani, G., Cecchi, A. and Tralli, A. (2014), "Full 3d homogenization approach to investigate the behavior of masonry arch bridges: the venice trans-lagoon railway bridge", *Constr. Build. Mater.*, **66**, 567-586.
- Smoljanovic, H., Zivaljic, N. and Nikolic, Z. (2013), "A combined finite-discrete element analysis of dry stone masonry structures", *Eng. Struct.*, **52**, 89-100.
- Tao, Y., Stratford, T.J. and Chen, J.F. (2011), "Behaviour of a masonry arch bridge repaired using fibre-Reinforced polymer composites", *Eng. Struct.*, **33**(5), 1594-1606.
- Toker, S. and Unay, A.I. (2004), "Mathematical modelling and finite element analysis of masonry arch bridges", *J. Sci. Gazi Univ.*, **17**(2), 129-139.
- Ural, A., Oruc, S., Dogangun, A. and Tuluk, O.I. (2008), "Turkish historical arch bridges and their deteriorations and failures", *Eng. Fail. Anal.*, **15**(1-2), 43-53.
- [URL-1]PEER (2013), Pacific Earthquake Engineering Research Centre, <http://peer.berkeley.edu/smcat/data>.